Polymeric Transcatheter Heart Valves

By

Johan Coetzee

SUBMITTED TO THE UNIVERSITY OF CAPE TOWN
In fulfilment of the requirements for the degree

MSc (Med) in Biomaterials

January 2019

Division of Surgery, Department of Cardiothoracic Surgery

University of Cape Town

Supervisors:

Assoc. Prof. D. Bezuidenhout

Dr. J. de Villiers

DECLARATION

I Johan Coetzé hereby declare that the work on which this dissertation/thesis is based is my original work (except where acknowledgements indicate otherwise) and that neither the whole work nor any part of it has been, is being, or is to be submitted for another degree in this or any other university.

I empower the university to reproduce for the purpose of research either the whole or any portion of the contents in any manner whatsoever.

Signature: Signed by candidate

Date: 11/2/2019

Abstract

Rheumatic heart disease (RHD) is one of the main causes of heart disease in the emerging world. Once the disease has become symptomatic valve repair or replacement is the only treatment currently available. Commercial bioprosthetic valves (surgical and transcatheter) suffer from calcification and decreased durability, especially when implanted into younger patients, while mechanical surgical valves require life-long anticoagulation. Polymeric transcatheter aortic valve insertion (TAVI) is proposed as a solution to provide long-term durability without the need for anticoagulation.

A manufacturing method involving the spray coating of polyurethane solutions onto valve moulds, pre-coating a TAVI stent with a polyurethane of higher durometer, and subsequently spraying the combination of the stent and the mould to form integral attachments of the leaflets, is described. Valves were tested for leaflet thickness distribution, hydrodynamic function and accelerated durability, and subsequently implanted in an acute ovine TAVI model as proof of concept.

Effective Orifice Area (EOA) >1.7 cm^2, regurgitation < 10% and transvalvular pressure gradient < 10 mmHg were achieved. Leaflet thickness correlated indirectly with the EOA and directly with transvalvular pressure gradient, but not regurgitation.

After iterative improvements in the manufacturing process, valves with average thicknesses ranging from 140 to 160 µm showed highest durability (>150 million, and up to 600 million cycles). Surface roughness was reduced by applying a final pure solvent coat. Implanted valves showed good function, with no apparent central or paravalvular regurgitation, perfusion of coronaries, and EOA greater than1.6 cm^2.

In conclusion, a polymeric TAVI valve made by a new manufacturing method showed durability up to 15 years equivalent in vitro, and good hydrodynamic function in vitro and in vivo. The devices hold many potential advantages in terms of automation and cost of manufacturing, as well as function and longevity.

Acknowledgments

Thanks to my supervisor Prof Deon Bezuidenhout for all the assistance as well as Head of Department Prof Peter Zilla. Dr. Jandre de Villiers, my co-supervisor, thanks for all the input and help. I would also like to thank Dr. Jacques Sherman for performing and the other staff that assisted with animal implants. Special thanks to Robin Smith for assisting with testing, David Conradie for helping where he could and Dr. Harish Appa for designing the moulds and stents used in this project. Finally, I would like to thank my wife, Lecia, for all the patience.

1 CONTENTS

List of figures

List of tables

BACKGROUND

1.1 NATIVE ANATOMY

1.1.1 Aortic valve

The heart consists of four chambers (the left and right atrium and the left and right ventricle) with four valves, the pulmonary, tricuspid, mitral and aortic valve (AV) that regulate flow between these chambers (Figure 1). This report will focus on developing a prosthetic replacement valve for the AV.

The AV regulates the blood flow from the left ventricle to the aorta. When the ventricle contracts (systole) blood is pushed through the valve into the aorta and when the ventricle expands (diastole) the valve closes to prevent blood from flowing back into the ventricle.

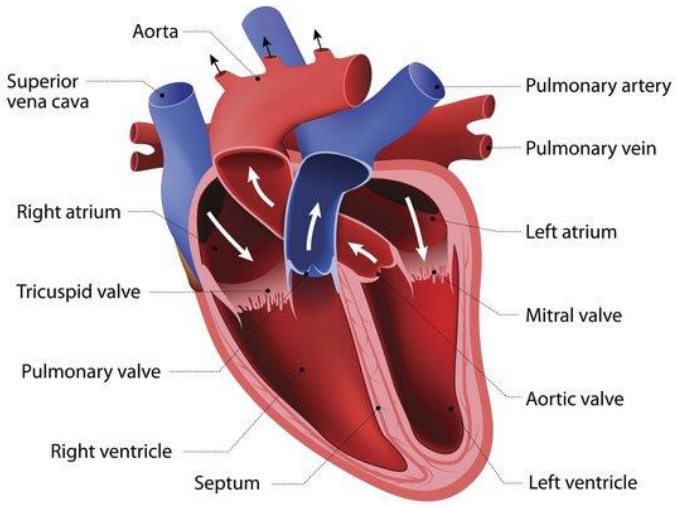

Figure 1 Schematic representation of the heart and the different chambers and valves found within[3]

Structurally the AV can withstand the extreme mechanical demands of opening and closing for billions of cycles. It consists of three layers, namely the fibrosa, spongiosa, and ventricularis (Figure 2). The fibrosa is situated on the outflow side of the valve, it provides the structural integrity needed for the valve to withstand the high back pressure of the blood. The middle layer is a soft 'sponge-like' layer that allows the other two outer layers to move relative to each other and in doing this takes up some of the stress on the valve. The final layer, the ventricularis, is on the inflow side of the valve and consists mainly of elastin, which is capable

of elongating and contracting for many cycles without losing its integrity. These three layers work in conjunction to allow the valve to function properly for extended periods.

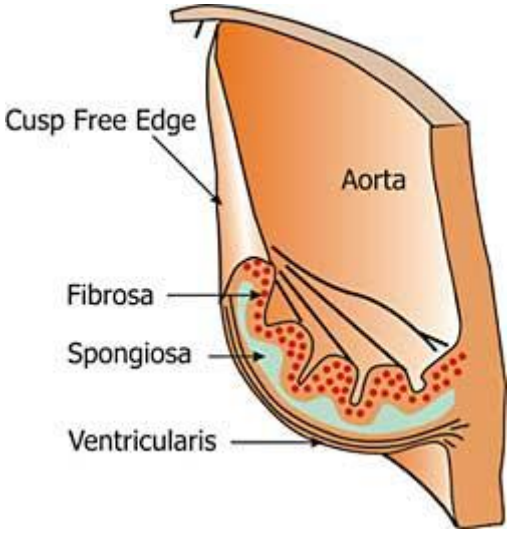

Figure 2 Representation of the native aortic valve and it's internal structure[4].

Each valve leaflet is a semilunar shape with a belly, free edge, and 2 commissures. The commissures are defined as the top of the free edge where the leaflet attaches to the aortic wall, the belly as the bulging middle part of the leaflet. Although the aortic valve is usually a tri-leaflet valve, abnormal bi-leaflet valves are seen in about 1-2% of people[5]

Calcification is the main cause of valve insufficiency in the developed world. Most individuals over the age of sixty have progressively enlarging deposits of calcium in their major arteries[6], which includes deposits on the AV. Moderate to severe calcification is present in 3% of people over the age of 75, with half of those diagnosed needing surgery[7].

1.2 Rheumatic Heart Disease (RHD)

In contrast to the developed world, the major cause of heart valve degeneration in the developing world is Rheumatic Heart Disease (RHD). Rheumatic fever is a disease that follows an infection of the throat (streptococcal pharyngitis)[8]. If left untreated rheumatic fever can then lead to the development of RHD, an autoimmune disease that inflicts damage to the heart muscle and valves. Unfortunately, in the developing world there are many people and communities who do not have access to antibiotics, which is the prescribed treatment for a streptococcal throat infection, and therefore many cases of RHD are seen in these countries. In a study covering 20 years, it was found that 65% of patients that contracted rheumatic fever developed RHD[9].

The conservative estimate of the global burden of RHD in 2005 was 15.6–19.6 million existing cases, with an approximate global incidence of 282,000 new cases per year[10]. RHD is the major cause of valvular heart disease-related mortality and morbidity in low- and middle-income countries[11] and some estimations have suggested that RHD causes 1.4 million deaths per year[12]. These statistics paint the picture for just how big a burden RHD is in the developing world and that a treatment that is accessible, affordable and effective is needed to improve their quality of life.

Although the availability of antibiotics is one way of preventing the spread of RHD, when it has developed beyond a certain point, prophylaxes are no longer effective and heart valve replacement or repair therapy is the only current treatment[13].

1.3 CURRENT TREATMENTS

There are two types of valve replacement options currently available, namely surgical and transcatheter aortic valve implantation (TAVI). Both surgical and TAVI replacement options are, however, inaccessible to patients in the developing world due to lack of medical facilities.

1.3.1 Surgical valve replacement

Surgical valve replacement is done by doing a thoracotomy (opening the chest), accessing the heart and excising the diseased valve and suturing in a replacement valve. This operation is very traumatic to the body and the post-procedural hospital stay is 19 days on average, while the cost of the entire treatment has been estimated to combine to a hefty R500 000[14].

Surgical valves can be classified into two different groups, bioprosthetic valves with leaflets made from animal or human tissue, and mechanical valves mostly made from pyrolytic carbon.

1.3.1.1 Mechanical valves

The first successful surgical aortic valve replacement was performed by Harken as early as 1960[15] (figure 3). After the initial success, mechanical valve replacement was adopted as a regular treatment for valve insufficiency.

However, the implementation of this technology was not without problems, where most notably, certain versions of the Bjork Shiley mechanical valve were recalled after being implanted in approximately 86 000 people[16].

Placing such a large foreign device inside the bloodstream also presents complications not only relating to mechanical durability, but the need for the patient to take lifelong anticoagulation drugs[17]. Although mechanical valves have extremely good durability and are able to last for billions of cycles, unfortunately taking anti-coagulation drugs carry detrimental side effects, as they increase the risk of fatal bleeding and have a negative effect on the quality of life of the patient[18].

Figure 3 St Jude Regent mechanical heart valve (Left) and Edwards Perimount aortic bioprosthetic valve (middle) and the first implanted mechanical surgical valve (right)

1.3.1.2 Bioprosthetic valves

Bioprosthetic heart valves are defined as valves made from tissue obtained from a biological source, including human, porcine and bovine. The tissue is usually treated chemically before implantation (fixation) to increase durability and biostability in vivo, which was first done by Carpentier in 1969[19] (an example of a commercial surgical valve, the Edwards Perimount can be seen in Figure 3).

The first commercially available bioprosthetic valve was the Hancock porcine valve that was implanted in 1970 and since then numerous valves have been manufactured and implanted over decades and developed into a multi-billion-dollar industry. The hydrodynamic function of a bioprosthetic valve mimics that of the native valve and the even flow dynamics allow the valve to function without the need for the patient to be on anti-coagulants as is the case with mechanical valves.

Bioprosthetic valve leaflets, however, tend to undergo structural deterioration[20]. Half of all tissue valves fail within 15 years of operation. The two main issues are calcification, which is accelerated in younger patients[21], and regurgitation due to tears in the tissue[22].

Table 1: Durability of Bioprosthetic valves in RHD patients[23]

Age	Durability
>70	15+ years common
> 20 & < 40	10+ years uncommon
<20	5+ years uncommon

1.3.2 Transcatheter Aortic Valve Implementation (TAVI)

Open heart surgery is very strenuous and frail patients are at high risk of experiencing post-operative complications from the procedure, with 77% of patients over the age of 90 experiencing complications[24]. This has led to 30% of patients with aortic stenosis no longer being considered as surgical candidates because of comorbidities and estimated surgical mortality risk[25].

A new development in heart valve replacement surgery, namely Transcatheter Aortic Valve Implementation (TAVI), was born from a need to address this. TAVI procedures are less strenuous on the body since the valve is inserted through a small incision and placed through a catheter. Recently, intermediate risk patients with severe aortic stenosis have also been considered for TAVI valve replacement[26].

Current commercial TAVI valves are made from bioprosthetic tissue that is mounted on a metal frame (stent) capable of being crimped and expanded. The valve is crimped and inserted through a catheter via different pathways to the heart. The main approaches for TAVI are summarized in Figure 4[27].

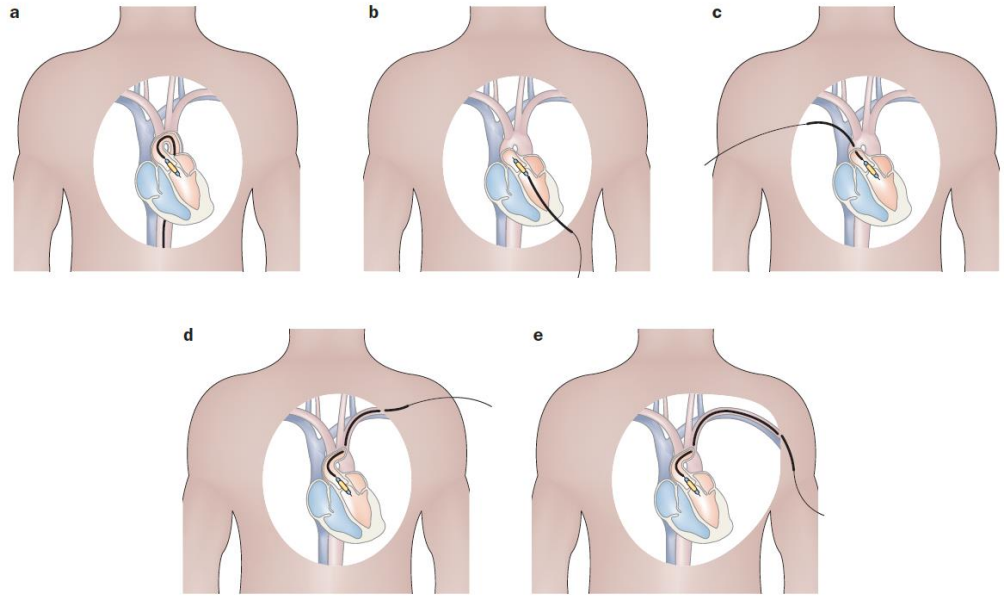

Figure 4 Different pathways used in minimally invasive cardiac surgery. A - Transfemoral, B - Transapical, C - Transaortic, D -Subclavian, E – Transaxillary.

1.3.2.1 TAVI history

Initial work on TAVI valves started as early as the 1960s[28], but it wasn't until the 1990s that Anderson et al[29] successfully implanted a transcatheter valve into pigs. This initial success led to several animal studies performed by different groups. Pavcnik et al[30] implanted a collapsible ball in cage valve into dogs in 1992 with negative results, while Bonhoeffer et al[31] and Boudjemline et al[32] successfully implanted valves in lambs and Lutter et al[33] performed short term studies in pigs.

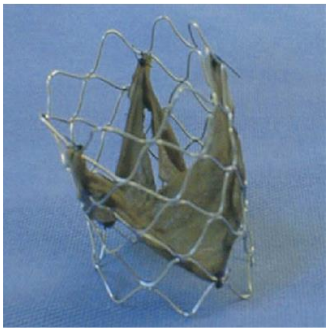

Figure 5 One of the first TAVI valves manufactured by Bonhoeffer et al[1].

After the initial animal trials, the first transcatheter pulmonary valve implanted into a human was done in 2000 by Bonhoeffer et al[34]. A bovine tissue valve was implanted into a young male patient and good valve function was reported directly after valve implementation.

The first TAVI was done by Cribier et al in 2002[35] and was made from bovine pericardium leaflets mounted on a balloon expandable stent. Good valve performance was still observed 4 months after implantation before the patient died due to non-cardiac related complications. After this initial case, another valve was implanted soon after via a retrograde approach through the femoral artery

by Paniagua et al[36]. Today TAVI procedures are standard procedure for high-risk patients with 180 000 implanted annually in the United States and Europe alone[37].

Currently, there are two TAVI valves approved by the FDA namely the Medtronic CoreValve and the Edwards Sapian valve and have been in use for almost a decade. More valves are currently available in Europe (Figure 6).

TAVI valves consist of two different types of valves, one type that is expanded from the crimped state using a balloon and another where the stent frame is made from a self-expanding shape memory alloy, usually Nitinol, called self-expanding valves.

All current commercial TAVI valve leaflets are bioprosthetic and thus will theoretically still be subject to the same challenges (discussed earlier) as the surgically implantable bioprosthetic valves when it comes to long term function in younger patients.

Figure 6 TAVI valves commercially available in Europe. (A) Edwards Sapien 3; (B) Medtronic CoreValve Evolut R; (C) Accurate neo (Boston, formerly Symetis); (D) JenaValve; (E) Portico Valve (Abbot, formerly St Jude); (F) Direct Flow Medical Valve; (G) Medtronic Engager Valve and (H) Boston scientific Lotus Valve[38].

1.4 Polymeric heart valves

Polymeric heart valves have the potential to exhibit the durability of mechanical valves combined with the hydrodynamic performance of bioprosthetic valves. Although work on polymeric valves originated many decades ago, they have not yet translated into clinical reality.

1.4.1 Surgical Polymeric Valves

The idea of making a synthetic replacement heart valve originated in the late 1950s. Mechanical and polymeric surgical valve replacements were developed at approximately the same time. The 3 main materials that have been considered for surgical polymer valve leaflets

are Silicone, Teflon, and polyurethane. Each material with the groups that investigated each is discussed below.

1.4.1.1 Silicone

Silicone is a very versatile material well known for its good durability and as such is used in a wide range of applications including adhesives, aeronautics, and pharmaceuticals[39]. The repeating unit in silicone is called a "siloxane" and one of the most common silicones is polydimethylsiloxane (PDMS) (Figure 7).

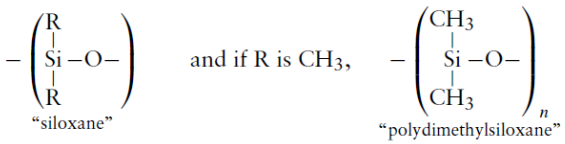

Figure 7 Structure of PDMS[39]

1.4.1.1.1 Surgical Silicone Valves

Roe et al used silicone as their material of choice to manufacture a polymeric heart valve[40] that showed good short term function, but subsequent sub-coronary implantation yielded unsatisfactory long term results[41]. The same group, after switching to a different silicone, clinically implanted their valves into 18 patients. Unfortunately, the study had a high mortality rate due to surgical complications and not due to valve failure[40].

Compression moulded Silastic valves were also made by Mohri et al. in 1972[42]. The valves performed well hemodynamically and mechanically, lasting 20 years equivalent function in a fatigue tester, but some variation was observed between different batches. Gerring et al. attempted fiber reinforced silicone valves, but an in vivo animal study found that 2 out of the 7 animals died due to thrombus formation in a 30 month study[43]. Chetta and Lloyd tested silicone valves in an accelerated fatigue tester, surviving up to 240 million cycles before failure[44].

One of the most prolific researchers developing polymeric valves in recent years is a group operating from Stony Brook University in New York.

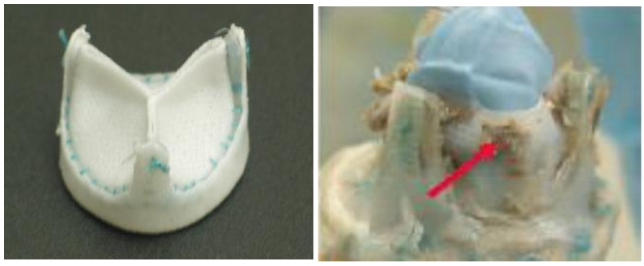

Figure 8 SIBS Dacron reinforced valve (left)[2], degradation in vivo of valve (right) 4

They started out by developing a polymer heart valve using poly(styrene-b-isobutylene-b-styrene) (SIBS) that incorporated polyester (Dacron) fibers into the soft polymer matrix (Figure 8). The material was selected due to its oxidative stability but had unsuitable mechanical properties, hence they initially reinforced the valve with the polyester fibres[45], after which the reinforcement was changed to polypropylene (PP) fibers. They focused on hemocompatibility and platelet activation tests were done to confirm the material's stability in a blood contact environment. In vitro tests concluded that the material had similar platelet activation to a St. Jude pericardial valve and that it could be possible to use the valve without life-long anticoagulation therapy. Durability issues associated with the modulus difference between the stiff PP reinforcement and the soft polymer matrix were observed[46].

Following the durability problems with the hard reinforcement within the soft matrix, the authors moved from a composite material approach to a single crosslinked version of SIBS called xSIBS. The material was deemed to have superior viscoelastic and creep resistant properties while keeping the blood compatibility of SIBS[47].

xSIBS is a thermoset and non-dissolvable material and cannot be processed using conventional solvent methods (like dip coating). An injection moulding system was thus developed for the manufacturing process (Figure 9)[48].

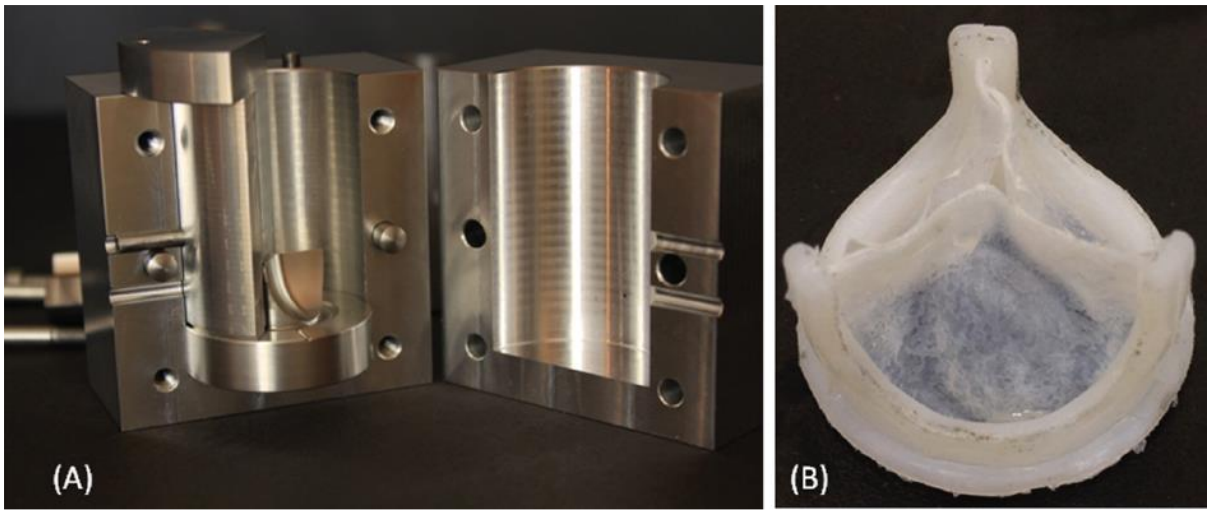

Figure 9 Stony Brook injection mould (left), with valve pictured (right).

The compression moulded valve was then tested in a pulse duplicator showing good hydrodynamic function (Table 2).

Table 2: PD data for the XSIBS TAVI and surgical valves [48]

	Mean ΔP	**Mean regurgitation fraction (RF) (%)**	**Effective Orifice Area (EOA) (cm^2)**
Reinforced sibs (19mm) [49]	14.4	3.24	1.14
xSIBS valve (19mm)	20.91	2.43	1.47

1.4.1.2 PTFE

Polytetrafluoroethylene (PTFE) is a material commonly known as Teflon. It is used in applications that require a chemically inert material and is used in a myriad of industries. Naturally, it was hypothesized that PTFE would carry its inert properties over to medical applications. Various groups have attempted to make valve leaflets out of PTFE with varying degrees of success.

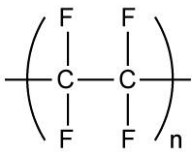

Figure 10 Chemical structure of PTFE

1.4.1.2.1 Surgical PTFE valves

In 1977 Imamura and colleagues[50] developed an expanded PTFE (ePTFE) surgical aortic valve. To compensate for the lack of strength of ePTFE, cross-directional laminated sheets were used to reinforce the valve. In vivo studies were done in 28 mongrel dogs and it was noted that good valve hemodynamic function was necessary to decrease thrombosis and optimal valve thickness should be chosen to prevent this. Thrombus formation and fibrin were seen on the valve surfaces.

Braunwald and Morrow[51] also manufactured a valve from PTFE fabric and clinically implanted it into 23 patients. The valves failed due to stiffening and tearing. A small amount of calcification was also observed. Nistal et al.[52] then investigated ePTFE for use as heart valve material and implanted their valves into sheep. They also observed stiffening and macroscopic calcification on the material.

1.4.1.3 Polyurethane

Polyurethane is one of the most promising alternatives to tissue for heart valve leaflets and its properties will be discussed in more detail than the other two materials due to it being the material of choice in this study.

Polyurethane is an organic polymer that was discovered by Otto Bayer in 1937. It is classified as a polymer containing a plurality of urethane groups in the polymer backbone, regardless of the composition of the rest of the molecule[53]. It is synthesized by reacting a di-isocyanate with a material that has hydroxyl functionality, usually a long chain diol, forming the pre-polymer. This pre-polymer is then traditionally reacted with a shorter chain molecule, called a chain extender. The chain extender reacts with the pre-polymer to form a long chain molecule made up of two distinct repeating units, referred to as hard and soft segments (Figure 11). The hard segment is defined as domains of alternating isocyanate molecules linked by a chain extender, while the soft segment is the long chain diols that were initially reacted with the isocyanate to form the pre-polymer.

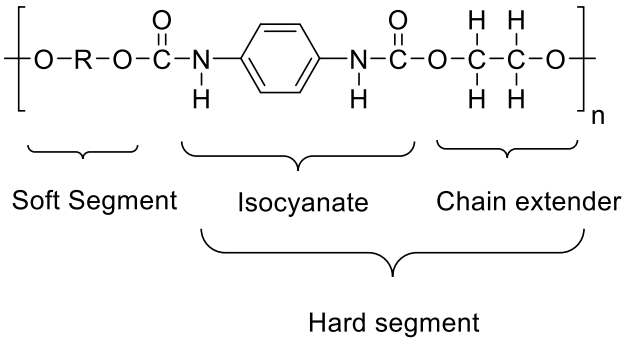

Figure 11 Typical structure of a polyurethane.

Polyurethanes are either a thermoset or a thermoplastic and can vary in stiffness, strength, hardness, chemical stability, and composition. This makes polyurethanes a very versatile material capable of being synthesized according to the intended application. This fact has led to a large demand for the material which was estimated to be $5 billion in the USA in 2010[54].

Although PU's can be mechanically strong, in vivo degradation was noted in early PU formulations that contained polyester soft segments[55]. Soft segments made from polyether and polycarbonate were then formulated to increase biostability. Poly-ether soft segments have since been shown to degrade via oxidation[56,57] using in vivo and in vitro models, while poly-carbonate based urethanes degrade via oxidation[58] and hydrolysis, although to a lesser

degree than ether or ester based urethanes[59]. One of the examples of a newer generation polyurethane is one with polydimethylsiloxane (PDMS) incorporated within their structure to further improve biostability.

1.4.1.3.1 Polyurethane mechanical properties

The mechanical properties of heart valve leaflet material are critically important. The modulus (stiffness) of a material has been linked to the hydrodynamic performance of a valve and it was found that the optimal material modulus should be below 60 MPa[70]. The ultimate tensile stress (UTS) and max strain are also two important metrics in classifying material properties. Table 3 lists the mechanical properties of a few polyurethanes used to manufacture polymeric valves[60].

Table 3 Mechanical properties of different commercial polyurethanes used in heart valves.

Polymer	Hardness (Shore A)	Tear Strength(N/mm)	Tensile Strength (N/mm^2)	Elongation at Break (%)
Estane (PEU)	85	55	48.3	570
Chronoflex C	80	45	37.9-45.5	400-490
Elasteon	75-90	50-80	20-30	500-750
POSS-PCU	84	50 ± 1.2	53.6 ±3 .4	704.8 ± 38

1.4.1.3.2 Surgical Polyurethane Valves

The first attempt at a surgical polyurethane valve was by Akutsu and colleauges[61]. They produced a valve by dip casting using a "virtually crosslinked" polyurethane with a thickness of about 120 – 180 µm, which they reported was the optimal thickness. The valves were implanted into dogs, most of which died within a few hours due to procedural complications, however, the ones that survived showed clotting on the valve surface.

Ghista et al.[62] dip coated an Avcothane valve and showed good hydrodynamic function in a pulse duplicator, but they did not publish any further studies. Wisman et al.[63] produced a surgical valve made by dipping a machined mould into a solution polymer dissolved in dimethylacetamide (DMAC). In vitro studies showed good valve function and in vivo studies were done in three different animal models, namely in calves, sheep, and goats. The valves showed a lack of calcification or thrombus in older animals but showed signs of both in younger animals.

Hilber et al[64] surgically implanted valves in the mitral position of 8 juvenile sheep. The implanted valves were made from Biomer, a polyether urethane urea. The valves were implanted for an average of 20 weeks, after which they showed signs of macroscopic calcification nodules, microscopic plaque-like deposits, fibrous sheaths and thrombotic material adherent to the leaflet surface. They postulated that surface morphology might influence the calcification of the valve. Kolff et al[65] manufactured valves that were implanted in sheep and showed no sign of thrombus but did show calcification.

The various studies mentioned above showed good in vitro function, but when it came to in vivo function the calcification and thrombosis were observed.

In the 1990s improved manufacturing techniques were available for valve fabrication along with newer polyurethanes that were specifically formulated to improve in vivo stability. Mathematical modeling and optimization of valve design were also being employed to design valves. However, after the disastrous clinical history of polymer prosthetic heart valves, the regulatory requirements made it more difficult to get clinical approval.

There were 3 main groups doing work on polyurethane heart valves at this time, they were groups based at Aachen University, Glasgow, and finally Leeds University.

1.4.1.4 Aachen University

Ruel et al[66] worked on a mono-leaflet reinforced polyurethane mitral surgical valve that showed good hydrodynamic function. Lo et al[67] continued the work by making dip cast polyurethane valves and implanting them into calves. The valves failed and caused the premature death of all animals. The reasons given were calcification, leaflet perforation, and thrombosis. They also hypothesized that calcification occurs before thrombosis, stating that calcification decreases leaflet mobility that causes thrombus formation to take place.

Jansen et al.[68] manufactured a polyurethane valve that was dip coated in a half-open position. The valve frame was manufactured from hard polyurethane, also dip coated, before the leaflets were moulded onto the frame. The valve showed excellent durability in accelerated fatigue tests, with valves reaching up to 648 million cycles. Apart from the half-open position, they also ascribed the valves good durability to the fact that the leaflets had a flat profile, which reduced the polymers shape memory effect.

A chronic bovine study in the mitral position of calves was performed with a bioprosthetic valve as a control. Six control valves and seven polyurethane valves were implanted for 150 days. Two animals implanted with the polymer valve died of non-valve related complications. The control explants had more calcification present on the leaflets than the explanted PU valves, however, thrombus formation linked to extrinsic calcification caused by surface roughness was observed on the polymer surface. They concluded that the valves performed better than the control valves, but further optimization is needed, particularly in improving the surface roughness of the valve.

After the work done in the 1990s, Deabritz et al. manufactured polyurethane valves for both the mitral and aortic positions[69,70]. The valve for the mitral position was made using a new manufacturing technique they called 'dropping' (Figure 12). This technique involved droplet deposition of polymer out of a nozzle controlled by a robotic arm akin to today's 3D printing technology. The valve was made from a polycarbonate urethane (PCU), said to be more stable than the previously used polyether urethane.

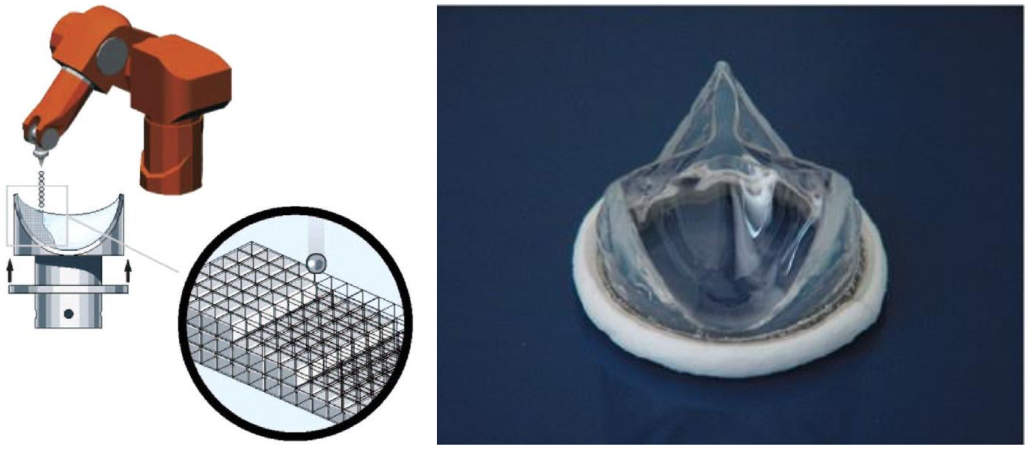

Figure 12 Illustration of the "dropping" technique used by the Aachen University group and a valve made by this group[66].

The mitral polymeric valve mimicked the geometry of the native mitral valve by having 2 leaflets. Perhaps the most impressive result was that this valve survived accelerated fatigue testing for up to 1 billion cycles, a number not previously reported for any valve. Six valves were implanted in the growing calf model where they outperformed commercial bioprosthetic surgically implantable prostheses. The commercial valves showed severe calcification and thrombus after the implantation period, where the PCU valve showed only mild calcification[69].

Perhaps more pertinent to this research project, the group subsequently published results for a 3-leaflet aortic valve also made using the dropping technique. They made the leaflets from 2 different PCU's of the same composition, but of differing hardness. A medium hardness PCU was used for the inside of the leaflets and softer PCU for the inner and outside faces of the leaflets. The leaflet thickness was extremely well controlled using the "dropping" technique and different parts of the valve were thicker than others to improve structural integrity at high-stress parts like the commissures while allowing for freedom of movement in the center of the leaflet. The thickness ranged from 80 – 200 μm[69,70].

The valves were implanted in the growing calf model in accordance with the group's previous valves[71]. The results were promising with five out of the seven valves implanted reaching the study endpoint. Two animals died due to pannus overgrowth at the valve inflow area. None of the control bioprosthetic valves reached the study endpoint due to valve failure related issues. A section covering TAVI polymeric valves later in this report will touch on Aachen University's most recent publications.

1.4.1.5 Glasgow University

The other main group performing polymer valve research from the '90s was Glasgow University. Bernacca et al. manufactured a valve by dip coating in polyether urethane[72]. The valves survived up to 307 million cycles in vitro, with the earliest failure at 21 million cycles due to a commissural tear. They concluded that these valves performed better than bioprosthetic valves but suffered from early mechanical failure. Improved thickness distribution and decreased surface roughness were cited as potential ways to improve the results.

A next version valve was then made on a mould with an elliptical-hyperbolic design. It was made by dipping the mould into a 35-45% w/v poly(ether)urethane (Estane) in DMAC solution, after which the sample was dried by suspending the mould free edge down after dipping[73].

One of the drawbacks of dip coating a polymeric valve was revealed in this study, namely the difficulty of controlling the thickness distribution within the valve leaflets. They reported valves with extreme variations within the thickness distribution when 16 different points were measured on a valve as seen in Figure 13.

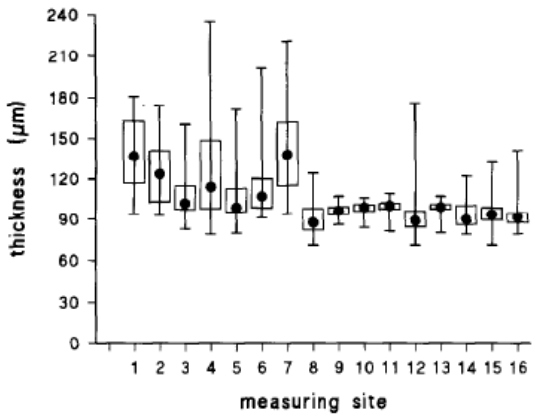

Figure 13. Thickness results from the dipping procedure used by Wheatley et al[73].

The hydrodynamic testing showed good valve function and good durability with six of the valves reaching over 470 million cycles.

The group subsequently changed to polyether-urethane urea (PEUE). Apart from the polymer, the valve design and frame remained the same as that used in the previous study[74] and the valves attained durability of up to 937 million cycles. Physiological calcification solution was used as the test fluid and some calcification was observed on the belly area of one leaflet, which consequently led to leaflet failure. The valves were mounted on a Polyether-etherketone (PEEK) frame and surgically implanted in the mitral position of sheep. Some extrinsic calcification was observed which might have been associated with material degradation as well as loss of hydrodynamic function associated with thrombosis[75]. It was also noted that the growing sheep model is a poor indicator for thrombosis.

The turn of the century marked the development and testing of a new, theoretically more biostable polyurethane called Elast-Eon, which is also a PEU, but which has silicone incorporated in the backbone of the polymer structure. There were two variations tested, one which was diol chain extended and one which was chain extended using a diamine, effectively making it a polyurethane-urea.

The thickness of the valves was, on average, just over 100 µm and was manufactured by dip coating onto a PEEK mandrel. The implantation was done in the mitral position of growing sheep and the valves were analyzed after 6 and 9 months of implantation. There was no evidence of thrombus formation, calcification or fibrin deposition[76].

After this study, the optimal Young's modulus and leaflet thickness for a polymeric heart valve[77] were investigated through hydrodynamic testing. The stiffness (S) of a material is

proportional to the thickness (b) and Young's modulus (E) with a relationship described by equation 1[78].

$$S = b^3 E \quad [1.1]$$

From this equation, the expectation was that the leaflet thickness would play a more significant role in the hydrodynamic function of a valve when compared to the material Young's modulus. Accordingly, the results confirmed this theory. Valves of similar leaflet thickness and different Young's modulus (up to 64 MPa) did not show significant pressure differences when tested in a pulse duplicator (Figure 14). They also stated that the use of higher modulus material would undergo less strain accumulation compared to lower modulus material, leading to potentially higher durability[77].

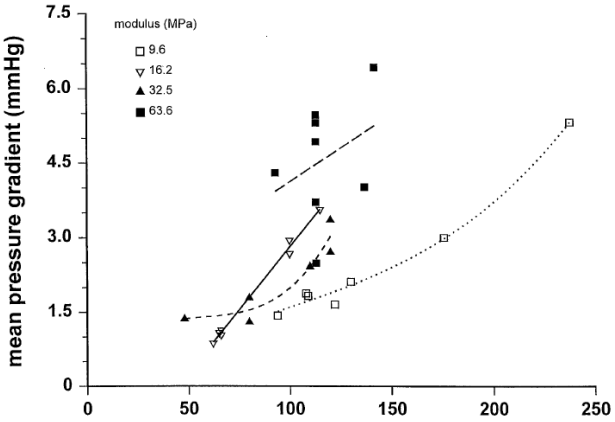

Figure 14 Effect of thickness and modulus on the pressure gradient of polymer valves

The group then compared leaflet thickness to the durability of the valve and found that for valves made from PEU, there seemed to be no correlation, indicating that there are other factors involved, but for PEUE valves the durability tended to increase with an increase in leaflet thickness[79].

Elast-Eon seemed like the perfect material for heart valve leaflets, but a later in vitro study suggested that the material lacked sufficient biocompatibility, which could only be increased at the expense of the mechanical properties of the material[80].

1.4.1.6 Leeds University

Important research in the field was also done by a group at Leeds University. They used a polyurethane called Eurothane, with an elastic modulus of 6 MPa which was dip coated onto

a PEEK surgical valve frame. The valve performed adequately in hydrodynamic tests together with 100 million cycles reported in fatigue tests. They also found that there was a sharp increase in the opening pressure of the leaflets with an increase in leaflet thickness[81].

They then compared two manufacturing methods, namely dipping and film fabrication[82]. Both methods used a "highly flexible" polyurethane with an elastic modulus of 7-10 MPa with 200 µm thick leaflets.

The hydrodynamic function of the two types of valves was similar, but there was a marked difference between the two techniques when it came to durability, with 4 of the film fabricated valves failing early before 30 million cycles, and two lasting up to 100 million. In contrast, however, all 6 dip casted valves reached 140 million cycles (the test endpoint) without failure (Figure 15).

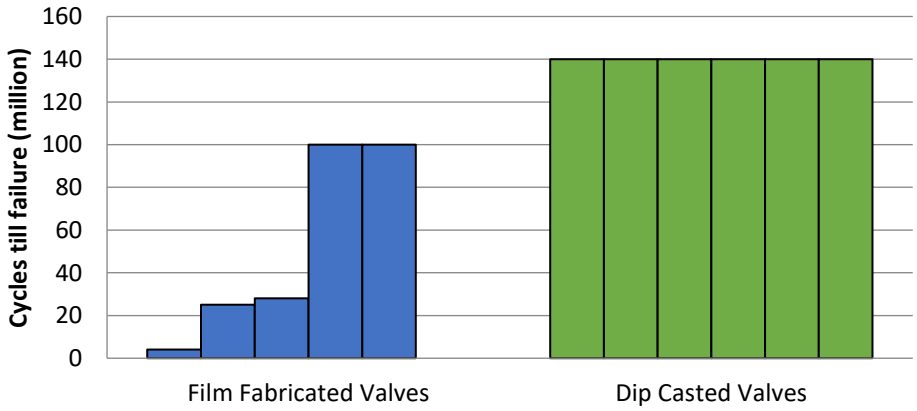

Figure 15 Durability of different manufacturing techniques (dip casted valves (green) reached study endpoint without failure)

This experiment highlighted the importance of the manufacturing methods used in fabricating polymeric heart valves. More specifically, they reiterated that the interface between the stent and the valve material is of critical importance for durability.

Fatigue testing of their valves at different rates found that there were differences in the opening and closing characteristics of the valve leaflets. They used image analysis to determine bending stresses and opening and closing times of the valves and found that at higher rates the valve was closed for less time during the valve cycle. They hypothesized that this might lead to false positive results[83].

1.4.1.7 University College London

A group at University College London (UCL) developed a novel polyurethane that incorporates polyhedral oligomeric silsesquioxane (POSS) nanoparticles. The POSS molecule (Figure 16) has a pendant chain with an alcohol functional group that is attached to the backbone of poly(carbonate-urea)urethane[84]. The material was tested extensively for its biostability and hemocompatibility, which includes anti-thrombotic potential[85], anti-calcification[86] and degrative resistance in vivo[87].

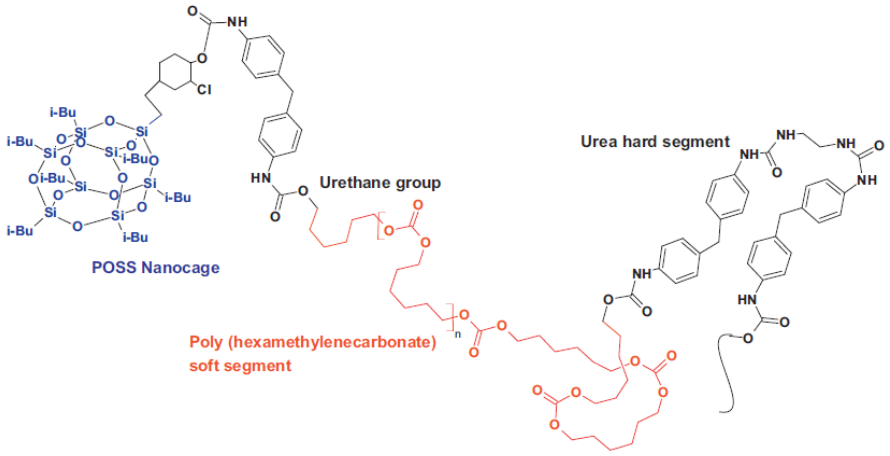

Figure 16 structure of the POSS-PCU polymer[84]

The UCL group developed a dip-coated surgical valve made from POSS-PCU[84] using an automated dip coating process. They manufactured valves of different thicknesses (Figure 17) and compared the hydrodynamic properties of each. The results indicated that the thinnest valve performed the best hydrodynamically with an EOA of 3.14 cm^2 and a 2.8 mmHg pressure gradient.

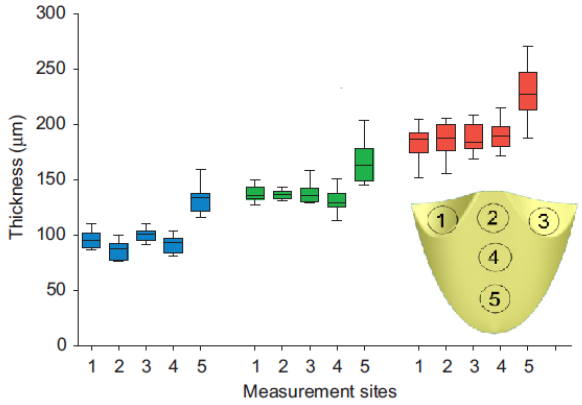

Figure 17 Thickness Distribution achieved by UCL group with their dip coating procedure (blue 100 µm average, green 150 µm average and red 200 µm average thickness valves).

1.4.2 TAVI polymeric valves

TAVI valves are currently used only in high or intermediate risk patients. There is a need to develop a TAVI valve that can be implanted into younger patients and polymeric TAVI valves have the potential to fulfill this need. The different groups that investigated polymeric TAVI valves are discussed below.

1.4.2.1 Institute for Clinical and Experimental Medicine, Czech Republic

One of the first examples of a polymeric TAVI valve was by Sochman et al. They made a tilting disc type valve that was mounted on a self-expanding stent (Figure 18). The stent was made from wire that supported a thin polyurethane tilting disc. The design was based on a valve proposed in 1965 by Davies et al[28] and adequate acute function was shown in dogs[88]. Another iteration of the valve was then developed and tested in an acute swine model and functioned adequately[89].

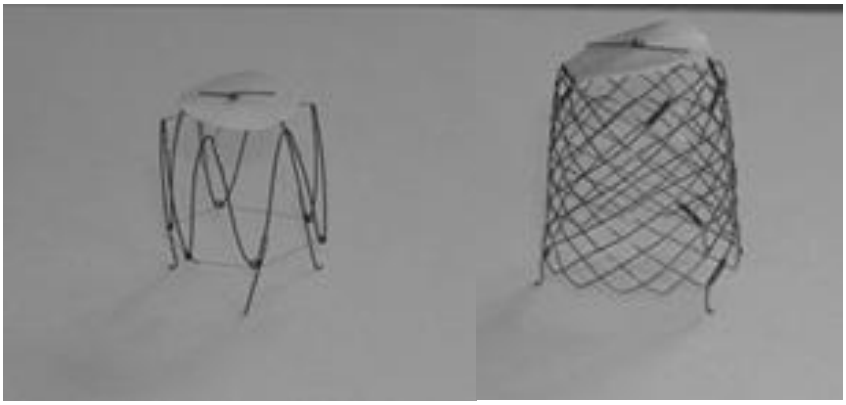

Figure 18. Two iterations made by Sochman et al. Left is the 1st valve followed by the 2nd valve on the right.

1.4.2.2 Tottori University

Another early example of a polymeric TAVI valve was made by Hashimoto et al[90]. Their valve (Figure 19) differed from the ubiquitous tri-leaflet design in that it had only a single polymer film attached in the center, allowing the valve to bend inward and allow blood to flow through.

The film was mounted on a self-expanding Nitinol frame that was repositionable and had a minimalistic nature in terms of being mostly stent material with a small polymer film attached at the edge. The minimalistic design decreased the possibility of coronary obstruction.

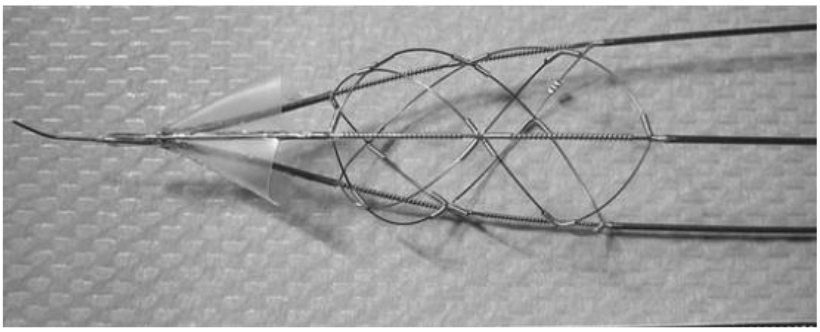

Figure 19. Hashimoto TAVI valve

The positioning and hemodynamic function of the valve was found to be acceptable in an ovine model. Thrombus formation was however observed at stagnant areas on the valve itself. The lack of outward force also rendered this valve incapable of treating stenosed aortic valves.

1.4.2.3 Christian-Albrechts-University of Kiel

A more conventional tri-leaflet polymeric self-expanding TAVI valve was developed by Attman et al[91] (Figure 20). The specific manufacturing details were not divulged, except that the valve was dip coated and the leaflet thickness was between 100-150 µm. The valve was tested successfully in the pulmonary position in a sheep model.

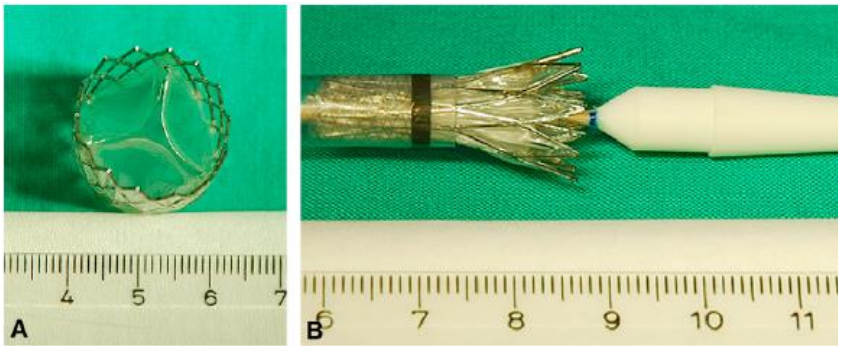

Figure 20 self-expanding TAVI valve from Attman et al.

1.4.2.4 Stony Brook University

Claiborne et al. at Stony Brook University developed TAVI valves initially using Dacron reinforced SIBS material[49], before switching to injection moulded xSIBS valves (Figure 21).

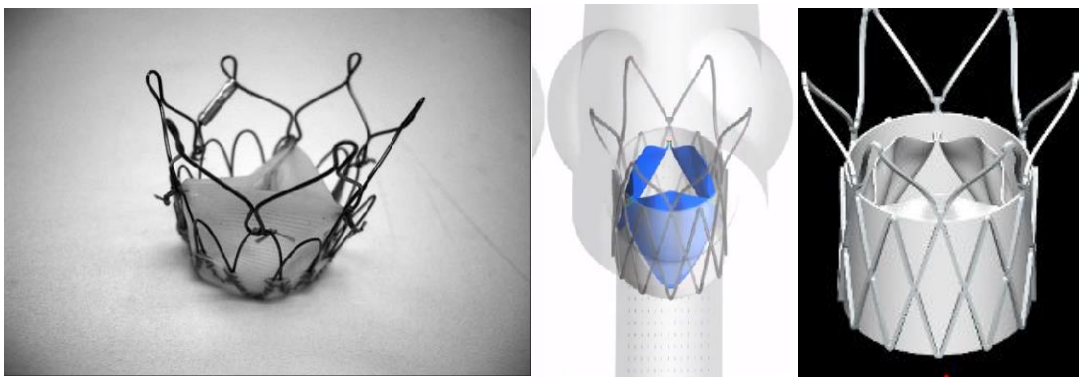

Figure 21 Reinforced SIBS TAVI valve (left), rendering of xSIBS TAVI valve (middle and right)

In recent years the group has expanded the scope of their research into different aspects of the valve. They investigated the thrombus potential of the valve, the optimum deployment position inside the anatomy[92] and heamocompatibility[93,94] amongst others, finding generally favorable results.

1.4.2.5 University College London

Having successfully developed a surgical valve that performed well hydrodynamically, Rahmani at al. (UCL) used POSS-PCU to make a dip coated, 130 ± 10 µm thick, TAVI valve (Figure 22) and compared it hydrodynamically to commercial TAVI valves (Edwards Sapian)[95].

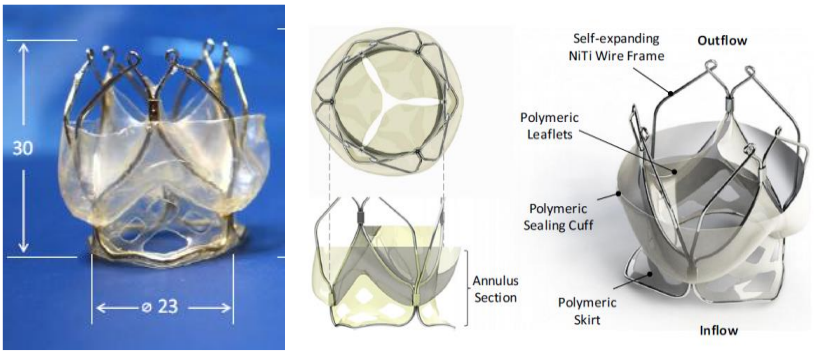

Figure 22 Left: UCL valve sample, Right: 3d model of valve.

The valves performed slightly worse than the commercially available equivalents, but still above ISO 5840:3 standard requirements, which is the ISO standard governing TAVI valve function, for all the three sizes of valves tested (Figure 23).

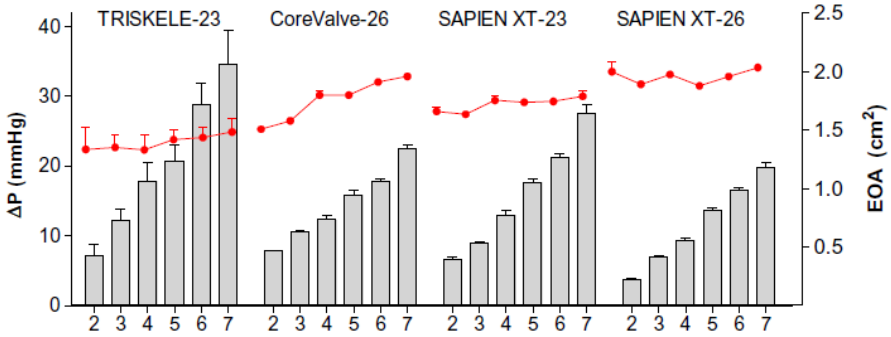

Figure 23 Performance of the UCL valve (Triskele) compared to commercial valves. The red line is EOA with values on right hand Y-axis, grey bars are pressure gradient, values on the left-hand axis. The X-axis represents L/min.

*1.4.2.6 **Second Military Medical University***

Zhang et al. made an ePTFE based transcatheter aortic valve (Figure 24), as PTFE valves have previously been shown to be subject to calcification[51], they proposed coating the ePTFE membrane in Phosphorylcholine. The valve was mounted on a balloon expandable cobalt-chromium stent and tested in an ovine model for 4 weeks in the pulmonary position. The valves showed good function and on explant, there was some pannus visible, but no thrombosis or calcification was seen[96].

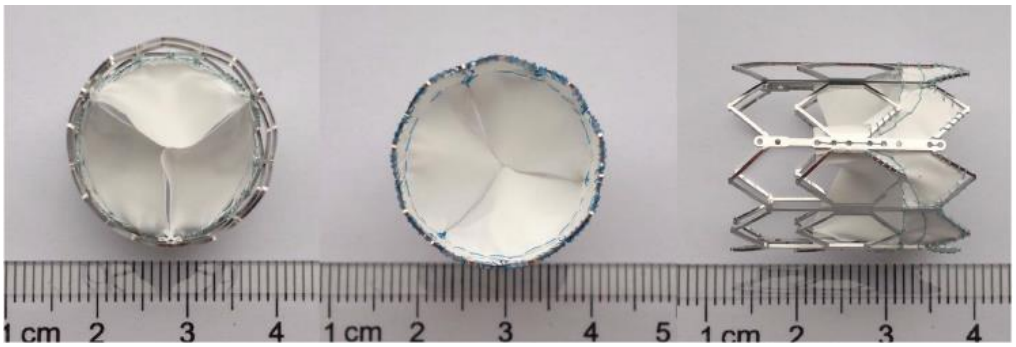

Figure 24 The balloon expandable ePTFE valve made by Zhang et al.

1.4.2.7 Aachen University

Wu et al. (Aachen University/Milan University) developed a TAVI valve using a 160 µm thick cylindrical polyurethane tube that was glued onto a self-expanding Nitinol stent (Figure 25)[97].

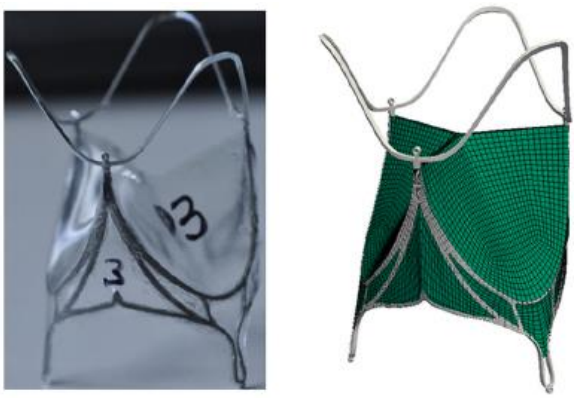

Figure 25 Aachen/Milan TAVI valve.

2 LITERATURE SUMMARY AND RESEARCH OBJECTIVES

RHD is an untreated global burden with many young patients in need of aortic valve replacement. Current surgical commercial valve replacement options are unavailable to these patients. TAVI valves could potentially be used to treat these patients but are also expensive and currently only suited to older patients due to valve durability issues.

Polymer valves can potentially be durable enough to implant into younger patients. Historically polymeric valves have suffered from a few problems that prohibited clinical adaptation, including durability issues, thrombosis, and calcification. Recent research has however seen renewed interest in polymer valves, including TAVI, due to new materials and manufacturing methods promising improved results.

This project forms part of a larger project that aims to provide an option for RHD patients by providing an affordable and durable TAVI valve replacement option. This study will focus on the optimization and characterization of the polymer valve itself by using a previously unused spray coating manufacturing method.

This thesis, therefore, has the following specific research objectives:

1. Manufacture valves using a custom automated spray rig.
2. Achieve good hydrodynamic function from the valves manufactured with performance exceeding ISO 5840:3 requirements.
3. Determine the relationship between leaflet thickness and hydrodynamic performance.
4. Manufacture an optimized valve that is capable of exceeding 150 million cycles before failure in durability testing.
5. Confirm good acute valve function in an ovine model.

3 MATERIALS AND METHODS

3.1 VALVE LEAFLET MATERIAL

The valve leaflets were made from a commercially available polyurethane, Carbosil®20 TSPCU (Carbosil 80A) (DSM, TE Heerlen Netherlands). It is a poly(carbonate)urethane with silicone incorporated in the soft segment. Biological tests done on the material (Table 4) confirmed biocompatibility.

Table 4 Biological test results obtained from the supplier. This shows that the material is suitable for use as a long-term implantable material.

Test	**Results**
Cytotoxicity	No evidence of causing cell lysis or toxicity
Genotoxicity:	In Vitro Chromosomal Aberration Non-genotoxic
Mouse Bone Marrow Micronucleus	Non-genotoxic
Muscle Implantation 2 weeks	Non-irritant
Muscle Implantation, 12 weeks	Non-irritant
26-week Carcinogenicity Study in the Transgenic ras H2 Mouse model	No increase in induced tumor formation
Hemolysis	Non-hemolytic
ISO Maximization Sensitization	No evidence of causing delayed dermal contact sensitization
ISO Intracutaneous Irritation	No evidence of significant irritation
USP and ISO Systemic Toxicity	No evidence of systemic toxicity
Chronic Toxicity, Subcutaneous Implant	No evidence of systemic toxicity
USP Pyrogen Study	Non-pyrogenic
Genotoxicity: Bacterial Reverse Mutation (saline extract)	Non-mutagenic
Genotoxicity: Bacterial Reverse Mutation (95% ethanol extract)	Non-mutagenic

3.2 SOLVENT

Dimethylacetamide (DMAC) is a widely used organic solvent and was used to dissolve polymers used in this study. All solution concentrations in this study are expressed as weight/weight percentage.

3.3 Effect of crystallization on mechanical properties

Mechanical properties of the valve leaflet material are integral to the performance and durability. After the polymer has been dried, the mechanical properties of the material still change over time due to polymer crystallization.

Carbosil 80A flat sheets were prepared by casting from a 15% solution of Carbosil in DMAC into a petri dish and drying in an oven at 60 °C overnight. From the flat sheet, tensile samples were stamped out on a press using a die that was made according to dimensions obtained from ASTM D638 Type C. The samples were then inspected for any defects and kept at room temperature. Testing was done by mounting the samples in custom made stainless-steel grips and extended at 12.5 mm/s until break at 2, 7 and 30 days (n = 5) using an Instron 5544 (Instron, Norwood, USA), equipped with a 500 N load cell.

3.4 Valve Manufacture

A specifically designed spray rig (Strait Access Technologies (SAT)) was used for valve manufacture.

3.4.1 Spray nozzle

The spray rig uses a 784S-SS aseptic nozzle (Nordson EFD, USA), along with a ValveMate™ spray controller (Nordson EFD, USA) (Figure 26). The nozzle on/off control and pressure settings were handled by the spray controller and the suggested pressure settings as supplied in the product manual were used, namely 1 bar air atomization and 0.5 bar liquid pressure.

Figure 26 The spray controller (left) and nozzle (right) used to spray valves inside the automated spray rig.

3.4.2 Spray Rig

The spray rig consists of two chambers, one for drying and one for spraying of the valves. The carousel (Figure 27) has the capacity for 8 moulds or stents and is positioned inside the drying chamber. The moulds/stents are then pushed into the spray chamber individually, coated, and retracted back into the drying chamber. The moulds/stents were rotated continuously while the process takes place.

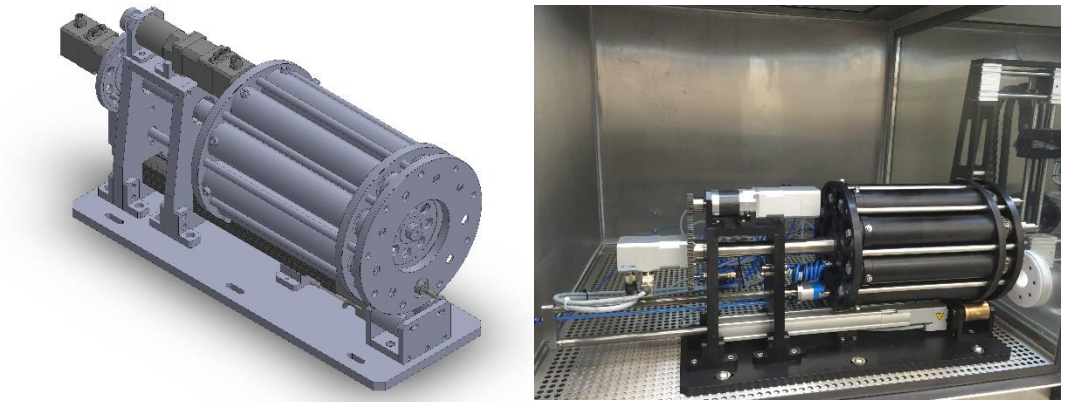

Figure 27 Carousel design file (left) and the finished carousel (right).

The nozzle position in the spray chamber was controlled using a gantry system (Festo, Germany) (Figure 28). Two linear rails (Festo, Germany) were mounted on a frame, one positions the nozzle in a horizontal direction and the other in a vertical direction. The nozzle was mounted on a stepper motor (Festo, Germany) that rotated the nozzle to the desired angle.

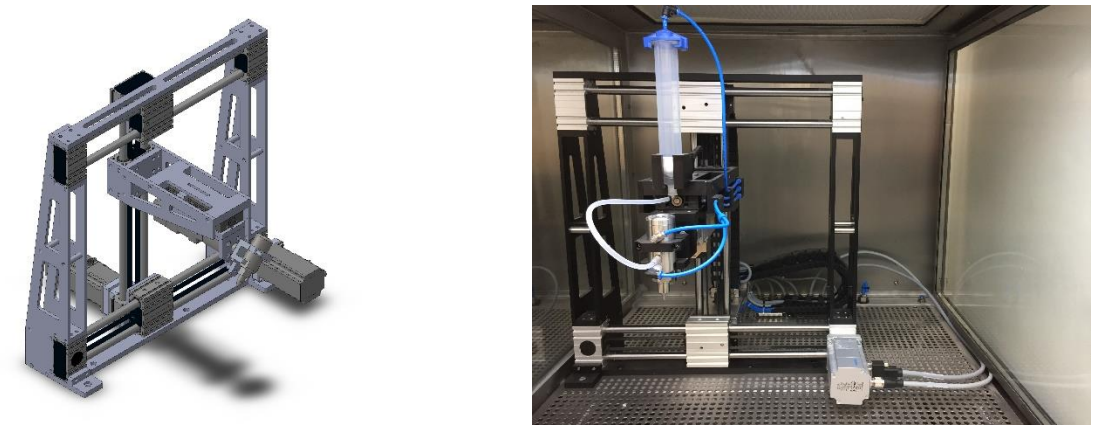

Figure 28 Nozzle gantry system design (left) and finished system (right). The gantry can position the nozzle at the desired spray distance and angle from the mould.

The control for both the spray and drying aspects was handled by a Siemens programmable logic controller (PLC) and the programming of the parameters could be done using a human-machine interface (HMI) (Festo, Germany) (Figure 29).

Figure 29 HMI used to program spray rig.

The HMI allows the user to program the horizontal (X) and vertical (Y) position of the nozzle, as well as the angle of the nozzle to the mould clockwise from perpendicular (Figure 30). From these parameters, the distance of the nozzle to the mould and angle of the nozzle from the mould can be calculated using basic trigonometry.

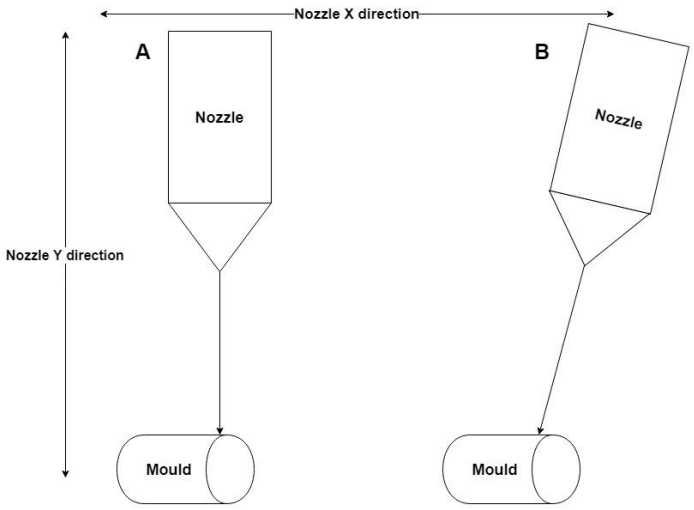

Figure 30 Schematic showing the nozzle at 0° (A) and at 13° to the mould (B).

The spray enclosure (Vivid Air, Cape Town) has two chambers separated by a glass panel, each with their own individual air circulation systems (Figure 31). The temperature and fan speeds are controlled using a programmable integral and derivative (PID) controller. The air is pushed through an activated carbon filter to remove any solvent vapors, then a High-efficiency

particulate air (HEPA) filter to remove any particulates, after which the air passes over a heating element and through the fan back into the spray/chamber.

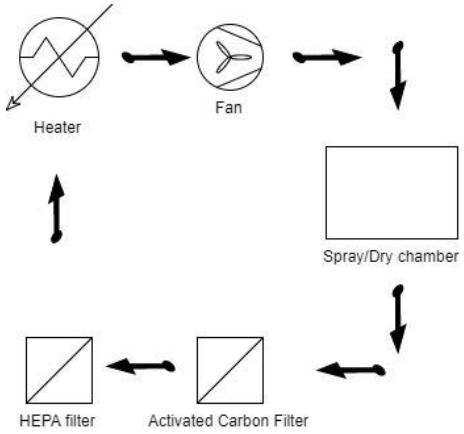

Figure 31 The environmental control loop within the spray enclosure.

3.4.3 Mould Pre-Coating

Custom moulds were made by a 3-axis CNC process according to an optimized valve design (SAT), pre-heated for 1 hour at 65°C in the drying chamber, before being pushed into the spraying chamber and sprayed for 6 s at a 13° angle and 130 mm from the nozzle using a 5% Carbosil in DMAC solution. The mould was then retracted back into the drying chamber and dried for 3 minutes before being coated again using the same parameters. The mould was always rotated at 20 RPM during the spray process, including when drying.

The nozzle was moved 20 mm in increments of 5 mm along the length of the mould, starting at the free edge and moving towards the nadir. At each increment 20 sprays were done, followed by drying at 65°C for 6 hours when all the sprays were finished.

3.4.4 Stent pre-coating

Stents (SAT) were pre-coated using a 4% Carbosil®55 TSPCU (Carbosil 55D) in DMAC solution. After pre-heating the stents for 1 hour at 65°C they were individually sprayed for 3 s and dried for 1 min between coats. The nozzle was also moved 20 mm along the length of the stents in 5 mm increments, with 40 sprays per increment and finally dried for 6 hours at 65°C.

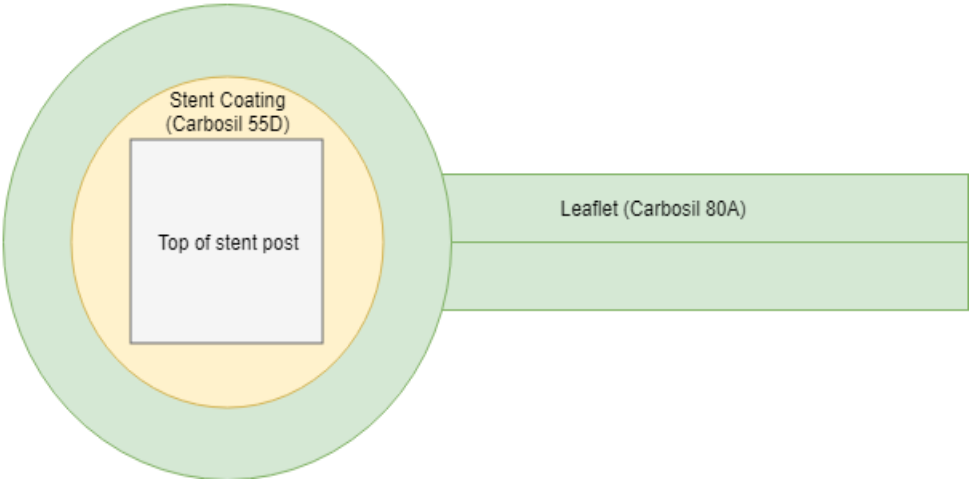

Figure 32: Stent (grey) coated in harder polymer Carbosil 55D (yellow), around which the softer polymer Carbosil 80A (green) extends as the leaflets.

3.4.5 Combination Coating

The pre-coated stent was then pushed over the pre-coated mould by hand. The combination of the stent and mould was then coated in the same manner as the mould. A summary of the parameters used in each step can be seen in Table 5.

Table 5 Spray parameters for different stages of manufacturing.

	Mould pre-coating	**Stent pre-coating**	**Combination coating**
Spray height (mm)	130	100	130
Spray duration (s)	9	3	9
Dry time between sprays (min)	3	1	3
Spray Angle (°)	13	0	13
Rotation speed (RPM)	20	20	20
Total number of sprays	100	200	100
Flow Rate (drops/s)	4	4	4
Number of sprays	40	160	40
Dry time after spraying (min)	360	360	360
Drying Temperature(°C)	65	65	65

For some valves in the durability testing section of this report, the stent was not coated. This will be mentioned in the relevant section.

3.4.6 Valve Removal

Valves were removed by swelling in water for 1 hour. An acetyl ring with an inside diameter (ID) ~0.25 mm bigger than the outside diameter (OD) of the mould was used to gently push the valve from the bottom up towards the edge of the mould until the valve slipped off.

Figure 33 Valve before being removed from the mould (left) and valve after removal and free edge cutting (right).

3.4.7 Leaflet Free Edge Cutting

The leaflet free edge was cut with small surgical scissors (Qosina, NY) along a slightly recessed line visible on the leaflets. The final valve after free edge cutting can be seen in Figure 33.

3.5 Valve Thickness Measurement

3.5.1 Digital caliper caliper

Valve thickness is integral to valve performance and durability. As such accurate thickness characterization is critical. Figure 34 shows the 13 points which were identified to be measured on each leaflet to give a good indication of the thickness across the entire leaflet.

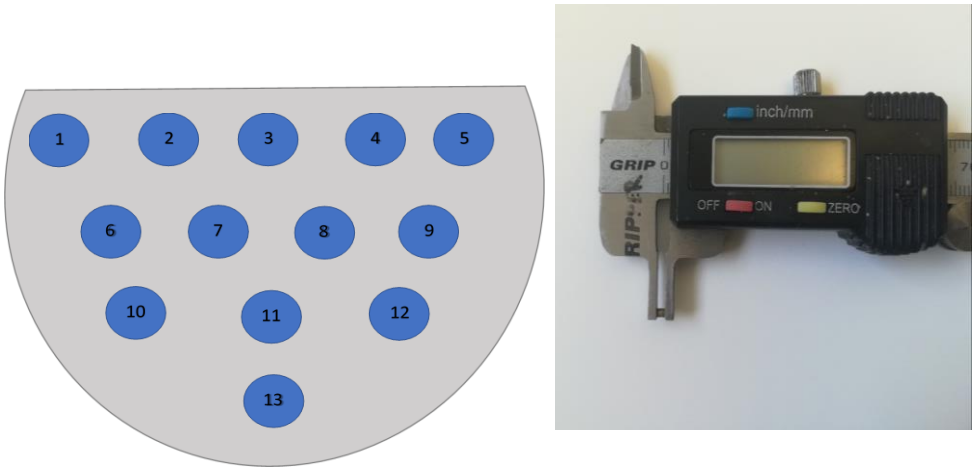

Figure 34 Measuring positions on valve leaflets (left) and modified digital caliper used to measure positions (right).

A normal digital caliper has a large measuring surface and the points that were identified were smaller than this surface. Thus, a digital caliper (Figure 34) was modified to be able to measure these points by machining the grips away and attaching two 0.5 mm diameter disks that press onto the part being measured.

Another thickness measurement technique used was non-destructive X-ray computed tomography (CT) (General Electric Sensing and Inspection Technologies/Phoenix X-ray (Wunstorff, Germany). The scanner contains two X-ray tubes, one tube with a reflection-type target and the other with a transmission target. The CT projects and captures an object from 360° and uses a dedicated computer algorithm to turn the image into a three-dimensional (3D) volume model.

Figure 35 Micro CT scanner used for valve thickness analysis (Left). The valve was mounted and is rotated 360° while acquisition takes place (right).

The 3D models contained some artifacts from interference caused by the metal stent. The artifacts had to be cleaned manually using open source 3D editing software Blender. The

artifacts were manually selected and removed while keeping the valve leaflet structures intact. The result of this removal can be seen in Figure 36.

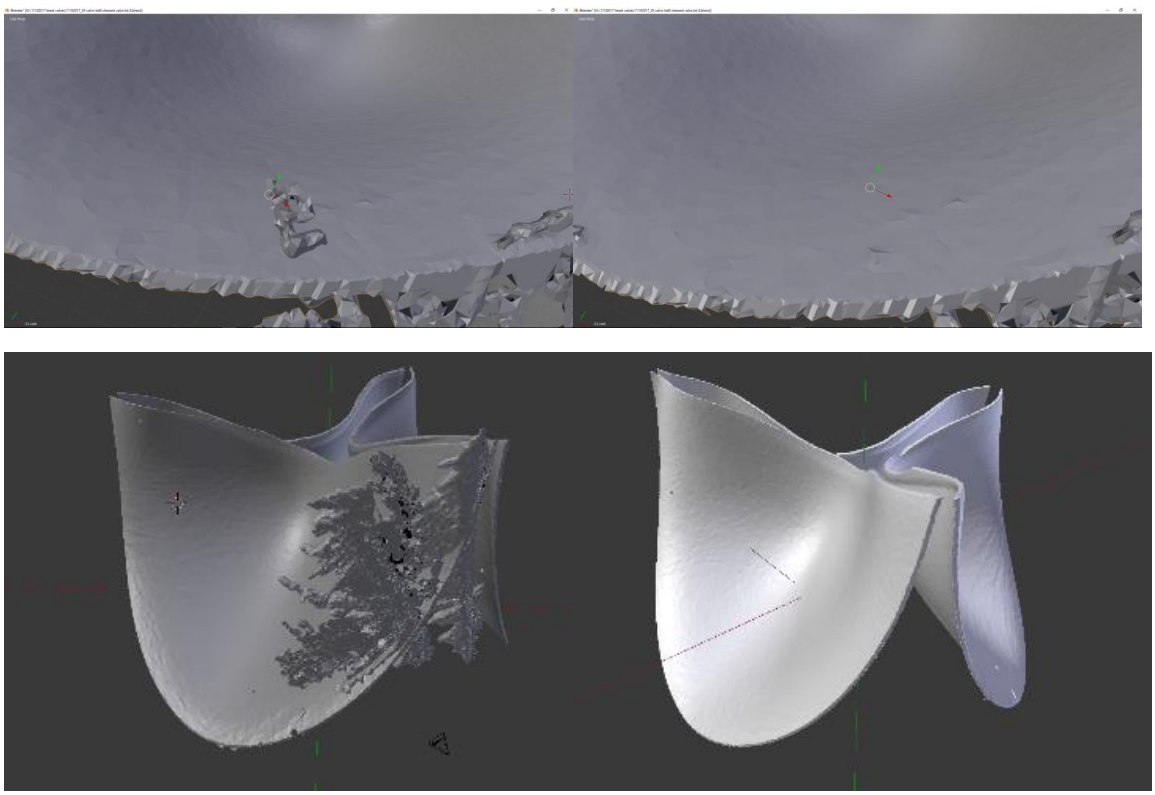

Figure 36 Manual artifact removal using Blender. Before (left) and after (right) after removing small (top) and larger (bottom) artifacts

After the artifact removal, the thickness of the leaflets was extracted, and a thickness histogram obtained from which an average could be extracted (full CT method).

A direct comparison of the thickness at the same 13 points was measured on the 3D model by manually selecting the same spots (13-point CT method). This was also done using Blender software (Figure 37).

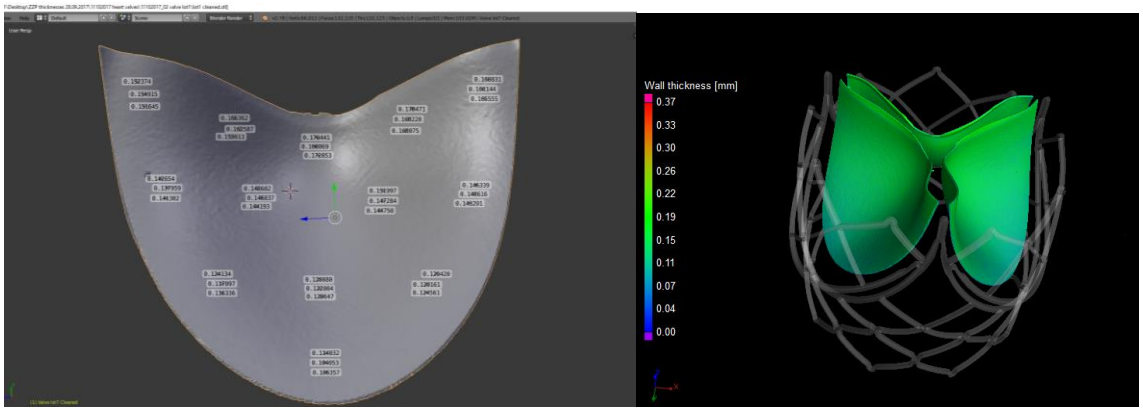

Figure 37 Manual measurement of pre-determined measuring spots from a 3d model (left) and model used for full CT measurement (right).

Valves (n=4) were sent for CT scanning to map the thickness of the entire valve, after which they were measured using the 13 point blender and digital caliper methods.

To check whether the 13 positions chosen accurately approximated the mean leaflet thickness and whether the Digital caliper measurements were accurate, a one-sample t-test was done comparing the 13-point CT and digital caliper to the full CT mean value. The one sample t-test was done on the assumption that the mean obtained from the full CT samples was the true mean of the valve leaflets. A confidence level of 95 % was used to assess significance ($p < 0.05$).

3.6 Sprayed leaflet evaluation

Sprayed valve leaflets (n = 8) were measured and the amount of thickness variation between measurement points and overall leaflet thickness variation investigated.

3.7 Hydrodynamic testing

To assess the hydrodynamic performance of valves they were tested using a Pulse Duplicator (PD) (ViVitro Systems Inc, Victoria BC) (Figure 38). The PD has a servo motor that pushes fluid periodically at physiological flow rates and set waveforms. The valve is mounted in a silicone ring inside a mock glass aorta.

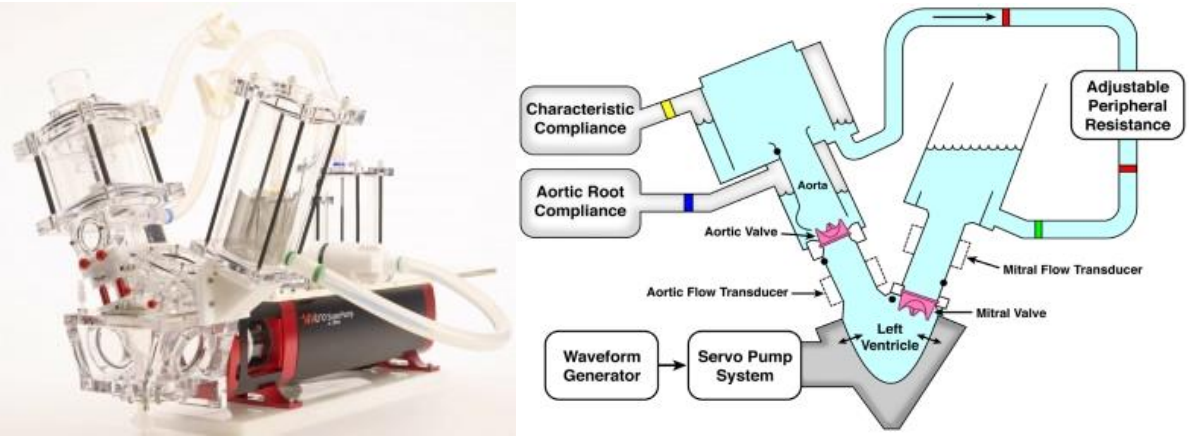

Figure 38 Pulse Duplicator used to test valves (left) with a schematic diagram of how it works (right).

From the PD, valve function can be estimated by evaluating different parameters, namely effective orifice area (EOA), mean pressure gradient (Δp) (pressure gradient) and the regurgitation. EOA is calculated using equations 3.1 and 3.3, the pressure gradient from equation 3.3 and regurgitation from equation 3.4. The testing fluid used in the PD was a 0.9% saline solution. The valves were tested at a flow rate of 5 l/m at a pulsatile rate of 70 BPM. 10 cycles of function were captured per sample and the mean was reported from these 10 cycles.

$$\boldsymbol{EOA}\ (\boldsymbol{cm^2}) = \frac{\boldsymbol{Q_{rms}}}{\boldsymbol{51.6}\sqrt{\frac{\Delta p}{\rho}}} \tag{3.1}$$

$$\boldsymbol{Q_{rms}} = \sqrt{\frac{\int_{t1}^{t2} \boldsymbol{Q(t)^2 dt}}{\boldsymbol{t_2 - t_1}}} \tag{3.2}$$

Where: Q_{rms} = Root mean square forward flow (ml/s), Δp = Mean Pressure Gradient (mmHg), ρ = Density (g/cm^3)

$$\Delta \boldsymbol{P} = \Delta \boldsymbol{P_o} - \Delta \boldsymbol{P_i} \tag{3.3}$$

Where: ΔP = Mean Pressure gradient (mmHg), ΔP_o = Pressure at outflow side of the valve (mmHg), ΔP_i = Pressure at inflow side of the valve (mmHg)

$$\boldsymbol{r} = \frac{\boldsymbol{V_c + V_L}}{\boldsymbol{V_T}} \times \boldsymbol{100} \tag{3.4}$$

Where: V_c = Closing Volume (ml), V_L = Leakage Volume (ml), V_T = Total stroke volume (ml), r = Regurgitation (%)

3.7.1 Valve thickness on hydrodynamic function

Valve thickness influences the mobility of the leaflets. To characterize to what extent this affects the hydrodynamic function valves with different thicknesses were assessed in the PD. Carbosil valves (n = 11) with different thicknesses were tested in the PD using the parameters described earlier.

3.8 Valve Durability Tester

Accelerated wear or durability testing was done on the valves to test the performance of the valves over time (Figure 39). This test involved running the valves at an accelerated rate of 15 Hz with a forward/backward flow ratio of 50% until failure using valve fatigue testers (FT) (BDC labs, CO, USA). Each FT has six independently operated test chambers which allows both displacement and frequency to be adjusted for each chamber. The testing fluid used was 0.9% saline solution.

Valve movement was visualized using a stroboscope. This was done by offsetting the strobe light frequency with the valve frequency by a small margin, the valve function can then be seen in “slow motion”. This allowed optimization of the resistance within the fatigue tester to maximize the valve opening area.

Figure 39 Valve durability tester (left) and Phenom scanning electron microscope (right)

3.9 Durability Optimization

3.9.1 Initial Valves

Initial valves (n = 3), were made by coating the mould as described earlier and then positioning the stent on the mould (without pre-coating), after which the combination was coated using the spray parameters seen in Table 5 and tested in the FT.

3.9.2 Matchstick

A polymer solution (15% Carbosil 80A in DMAC) was dropped onto the commissure post of the stent (called matchsticking from here onwards) using a pipette prior to valve manufacture to create a thicker polymer layer at this point (n = 6), otherwise, the valves were made in the same manner as the initial valves and tested in the FT.

3.9.3 Hard polymer coating

Stents were pre-coated as described earlier and valves (n = 6) made using the pre-coated stents as described earlier. They were then tested in the FT.

3.9.4 Decreased mould diameter

Pre-coating the stent and mould meant that the stent required a lot of force to position over the mould. A mould was made with a slightly decreased diameter (22 mm from 23 mm). To test whether this new mould design increased valve durability, valves were manufactured from the 22 mm moulds (n = 10), also incorporating the hard stent pre-coating, and tested in the FT.

3.9.5 Role of thickness on durability

To determine the optimal thickness for fatigue resistance, a retrospective study was done using fatigue results (n = 92, valves not part of this study, but manufactured in the same manner for tests outside the scope of this project, was also included). The valves used for the holistic analysis were from different stages in the optimization steps and includes valves without pre-coating, with pre-coating and valves made on smaller moulds with pre-coating.

3.9.6 GOA comparison

To confirm whether valve function was similar in the fatigue tester and the PD, video footage of a valve in both these machines was taken and used to calculate the geometrical opening area (GOA). The first frame of each video was taken, a circle drawn manually around the valve,

after which the diameter of this circle was assumed to be 22 mm (the inside diameter of the valves used). Thresholding was then used to discern the area of the valve that is open and the frame with the largest area was used from each video for calculations (Figure 40). This value was then used to calculate the GOA using equation 3.5. Java was used to write the software to do this.

$$\boldsymbol{GOA} = \frac{\boldsymbol{A_o}}{\boldsymbol{A_T}} \times \boldsymbol{\pi r^2} \quad (3.5)$$

Where: A_o = Amount of pixel within the open part of the valve, A_T = Total pixels of the valve area, r = radius of the valve (1.1 cm), GOA = Geometrical opening area (cm^2)

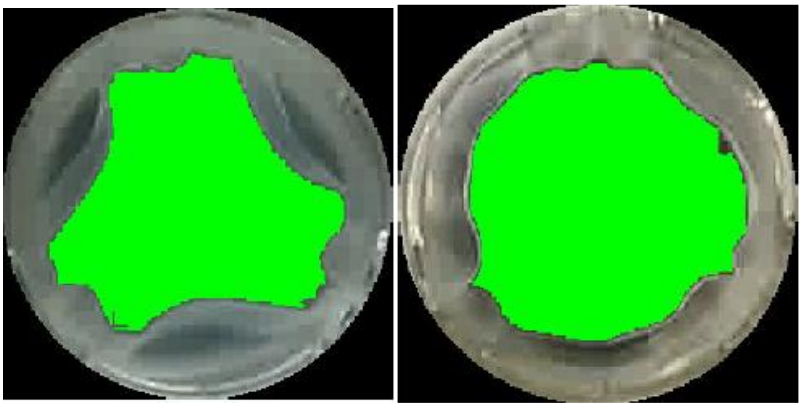

Figure 40 Representation of the maximum opening area for a valve in the FT (left) and in the PD (Right).

Valves (n = 4) were tested at 5 l/m and 70 bpm in the PD and at 120 mmHg in the FT. The difference in maximum area between the two machines was calculated according to equation 3.6.

$$\%\ \boldsymbol{GOA\ difference} = \frac{\boldsymbol{GOA_{PD} - GOA_{FT}}}{\boldsymbol{GOA_{FT}}} \times \mathbf{100} \quad (3.6)$$

3.10 Surface Roughness

The surface roughness was measured and compared for valves made by dip coating and spray coating. The spray samples (n = 3) were made using the same spray parameters as with valve manufacture (without the stent), while dip coated samples (n = 3) were manufactured by dipping a mould into a 20 % w/w Carbosil 80A in DMAC solution by hand, then drying the sample in an oven at 65°C overnight.

Scanning electron micrographs were taken using a Phenom XL scanning electron microscope (SEM) (Phenom, Eindhoven) (Figure 39) and a Jeol 5410 (Jeol Ltd, Tokyo). Surface roughness

calculation was done by using SEM images obtained from the Phenom. The outflow (side not in contact with the mould when manufacturing) and inflow parts of the leaflet were investigated.

There are two main variables that define surface roughness, namely arithmetical mean roughness value (Ra) and mean roughness depth (R_z). R_a is the average of the absolute values of the peak heights over the evaluation length, while R_z is defined as the average value of the absolute values of the heights of the five highest-profile peaks and the depths of five deepest valleys within the evaluation length.

3.10.1 Final solvent spray

A final solvent only spray was done after standard valve manufacture. Three samples were made, a control, 3x solvent sprays, and 5x solvent sprays. The valves were made in the automated rig with the standard spraying parameters on 22 mm moulds, except solvent only was sprayed onto the moulds using the same spraying parameters as with the polymer solution. After manufacturing, the valves were dried for 3 hours at 65°C, left at room temperature for 24 hours, gold sputtered, and analyzed using SEM.

3.11 Animal Trials

Animal trials were conducted according to UCT animal ethics guidelines under animal ethics number AEC 016/015.

To confirm adequate acute valve function in vivo, a valve was implanted into the aortic position of a 37.8 kg juvenile sheep. The sheep aortic annulus size was first determined on the farm using echocardiography before any procedures were done. If the annulus size was below 19 mm the sheep was brought to the animal housing facilities of the UCT animal unit and put on antibiotics for 10 days.

The sheep was then anesthetized, weighed and shaven. EKG monitoring was connected, and a transesophageal echo probe inserted. A mini-thoracotomy was then performed by a qualified cardiothoracic surgeon and Heparin administered. A pigtail catheter was positioned pre-operatively above the valve through the femoral artery, this was used to inject contrast in order to visualize the valve function under fluoroscopy.

The valve used in the acute trial had an electro spun skirt incorporated, this process does not fall within the scope of this project, but briefly, Carbosil 80A was electro spun from tetrahydrofuran and dimethylformamide, then bonded onto the outside of the valve using a soldering iron set at 200°C. The valve was then crimped (Figure 41) onto a non-occlusive deployment device (SAT) and inserted through the apex of the heart. The TAVI valve was positioned across the native valve and deployed after positioning was confirmed using fluoroscopy.

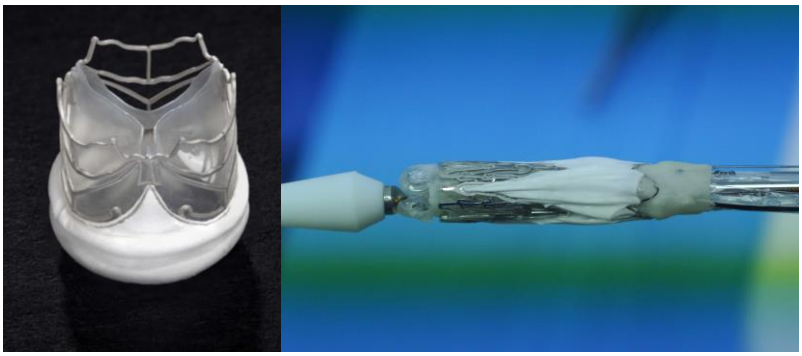

Figure 41 Uncrimped valve (left) and the valve crimped onto the deployment device (right)

Echocardiography (echo) measurements were done before, directly after the procedure and 3 hours after deployment to confirm valve function, as well as a contrast injection under fluoroscopy to confirm that the valve seals and that the coronary arteries were open. The sheep was then euthanized, after which the chest was opened using a bone saw and the heart removed. The valve was then carefully excised and photographed.

To test whether the valve function improved over time while functioning at 37°C, a valve from the same batch used in the animal trial was tested in the PD at 37°C for 3 hours at 5 l/m and 70 bpm. Measurements were taken every 30 minutes.

3.12 Statistical Methods

All comparisons were done using a student's two-tailed T-test, two-sample unless specified otherwise. A p-value of < 0.05 was considered statically significant. R^2 was used to quantify how well the data was correlated.

4 Results and Discussion

4.1 Polymer Crystallization

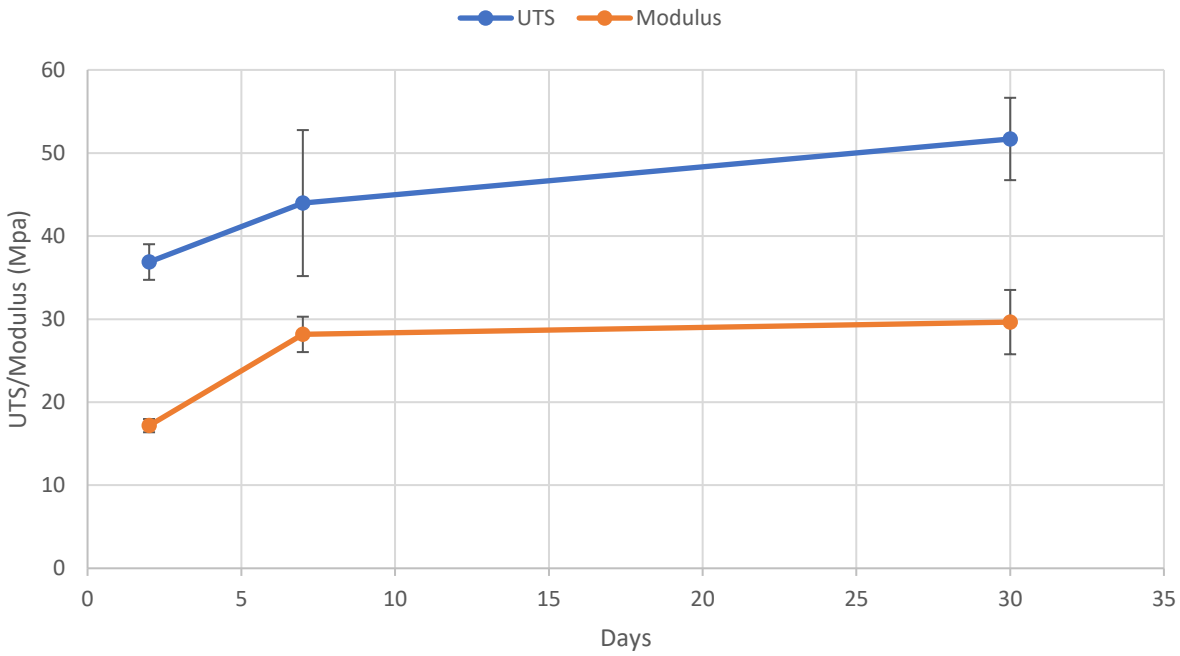

Figure 42 Change in mechanical properties over time.

Over 7 days an increase from 17.1 to 28.1 MPa ($p = 0.0009$) (Figure 42) could be seen in Young's modulus, but at 30 days was slightly, but not significantly ($p = 0.47$) higher at 29.6 MPa.

The UTS also showed an increase, but with the 7-day samples showing a large standard deviation (8.8 MPa). At 30 days, however, there was a significant increase compared to day 1 (37 vs 51 MPa, $p = 0.0014$).

These results showed that over time the polyurethane Young's modulus and UTS will increase due to crystallization of the material.

4.2 Thickness Measurement Validation

The average leaflet thickness measurement of each valve was slightly smaller using the digital caliper when compared to the full CT average (on average 7.83 ±2.7 µm less across the 4 valves) (Figure 43). The same was true when the digital caliper was compared to the 13-point CT, except for valve 1 where the digital caliper measured slightly larger (142 µm to 138 µm)

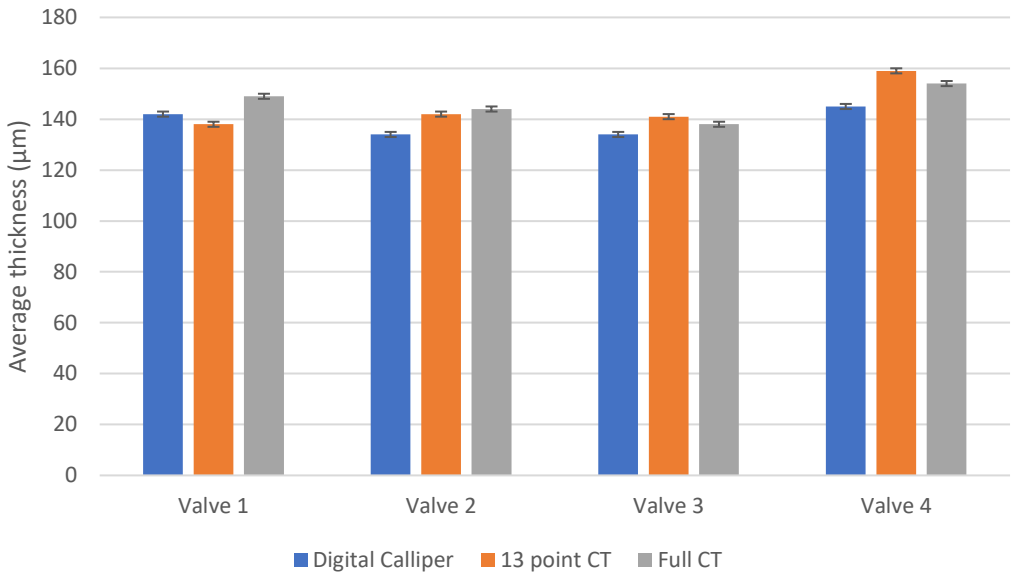

Figure 43 Comparison between measurements done using the Digital caliper, 13-point CT and full CT.

It was seen that the mean leaflet thickness measured using the 13-point CT were not significantly different from the full CT data for 3 of the 4 valves (Table 6), but the digital caliper means were found to be significantly different from full CT in all the samples.

Table 6 P-values comparing digital caliper and 13-point CT to full CT scan mean.

1 sample T-Test P compared to the mean from a full CT scan.		
	13 Point CT	**digital caliper**
Valve #	**P value**	**P value**
Valve 1	0.222	<0.0001
Valve 2	0.205	<0.0001
Valve 3	0.096	<0.0001
Valve 4	0.002	<0.0001

The fact that the 13-point CT method measurement did not significantly differ from the full CT average for most of the valves, indicated that the 13 points chosen accurately approximated the valve leaflet thickness. The digital caliper measurement, however, showed a significant difference from the full CT mean values, which means the Digital caliper measurement itself did not accurately approximate the mean leaflet thickness of the valves.

The Digital caliper measuring consistently thinner than the full CT mean values was due to the compression that takes place when doing measurements with the digital caliper. The difference was below 10 µm of the CT scan results and was deemed an acceptable difference

given the advantages (ease of use, affordability) of the digital caliper and was used for measurements in this study.

4.3 Valve thickness consistency

The valves made had an average thickness of 137.6 µm ± 16.6 µm. Variation between different positions on the valve was observed (Figure 44), with the center of the free edge (positions 2, 3 and 4) being the thickest (157, 150 and 147 µm), while the thinnest area was position 9 (127 µm) on the right side of the belly.

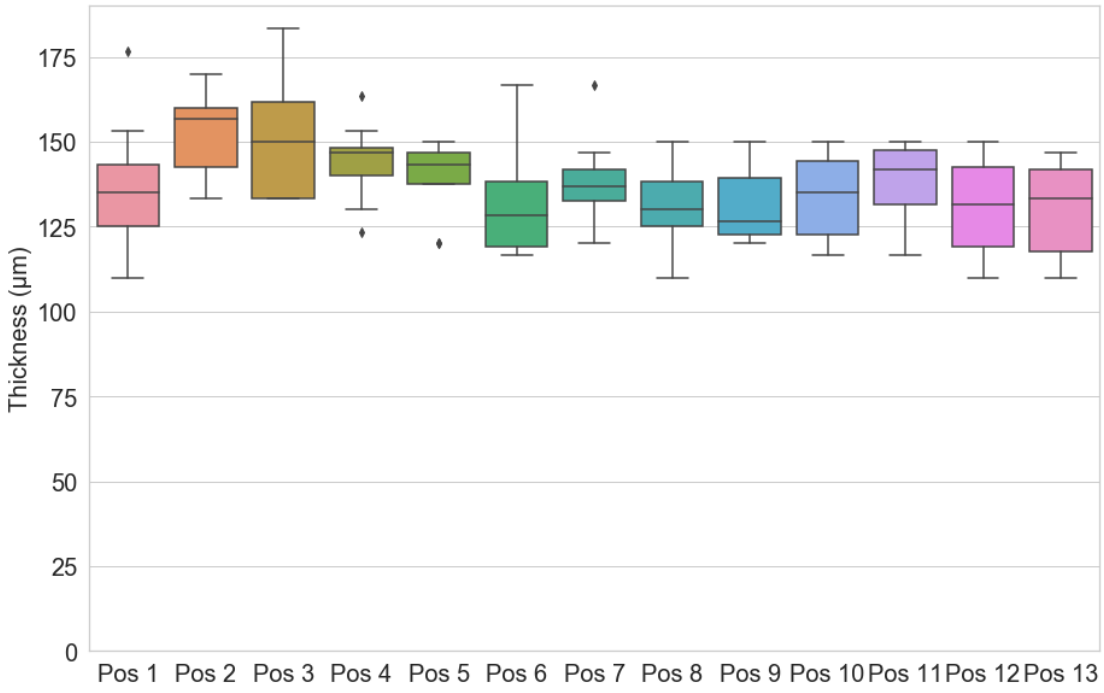

Figure 44 Thickness ranges for different parts of the valves.

4.4 Hydrodynamics

4.4.1 EOA

The EOA for different thickness valves varied from 1.48 to 1.81 cm^2 (Figure 45). As the thickness of the valves increased there was a tendency for the EOA to decrease. A trendline was drawn with a R^2 value of 0.85 ($p = 3.6$ E-07), indicating that there is a significant indirect linear relationship between thickness and EOA.

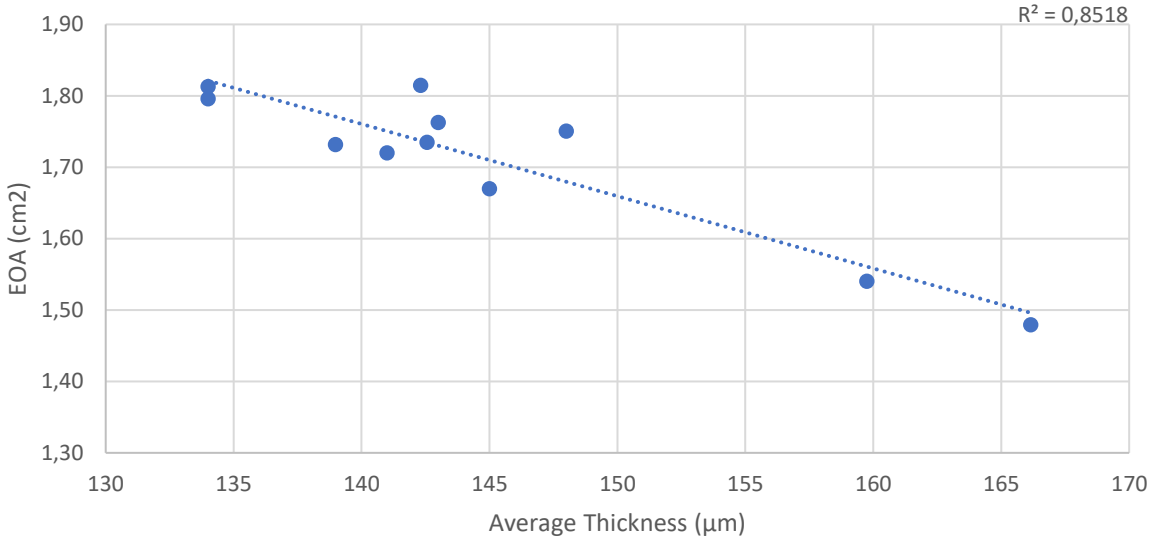

Figure 45 Effect of thickness on EOA

EOA values for all thickness valves were well above the ISO-5840-3 (2013) requirement for 23 mm valves of 1.2 cm^2.

4.4.1 Pressure Gradient

A correlation (R^2 = 0.82, p = 1.6 E-06) between pressure gradient and thickness of valve leaflets (Figure 46) was observed, indicating a significant direct linear correlation between the two. The maximum pressure gradient was 11.52 mmHg and the lowest observed was 8.05 mmHg.

This result is as expected as thicker leaflets will take more energy to open and thus cause an increase in pressure gradient and agrees with literature[81]. The EOA and pressure gradient follows the same trend and is influenced by the same parameters, due to pressure being used to calculate both.

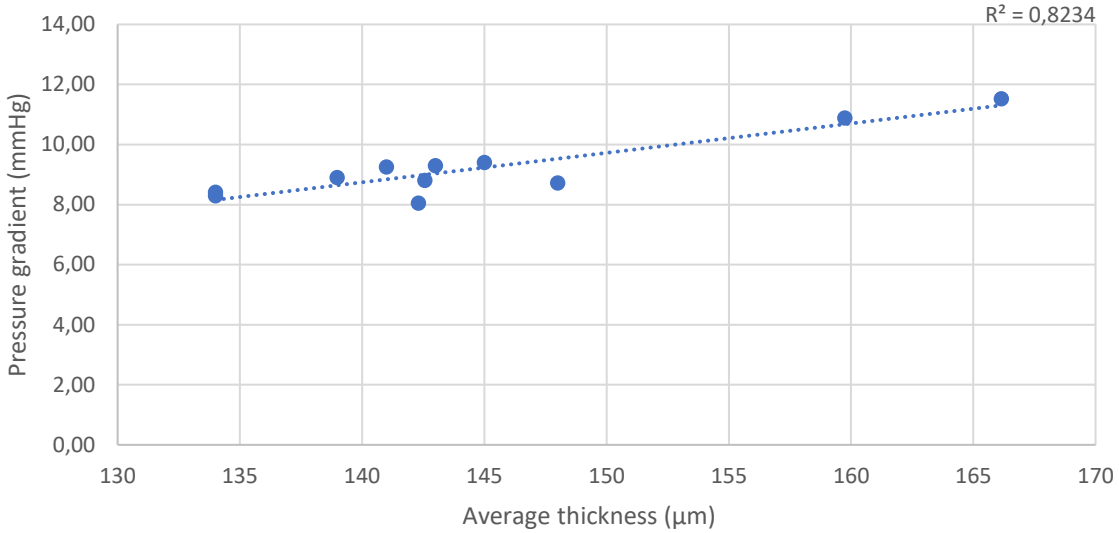

Figure 46 Average thickness vs pressure gradient

4.4.1 Regurgitation

Unlike EOA and pressure gradient, there was no correlation between regurgitation and leaflet thickness (R^2 = 0.027, p = 0.91) (Figure 47). The highest regurgitation observed was 20.51 %, while the rest of the valves showed regurgitation below 10 %.

Most of the valves, except for 1 outlier (20.51 %) had regurgitation below the ISO 13485:3 standard of 20%. Inconsistency in free edge cutting could possibly explain this outlier.

The fact that there was no correlation between regurgitation and thickness was a bit surprising as thicker leaflets would intuitively take longer to close and as regurge is calculated by adding the closing and leakage volumes, thicker leaflets should then intuitively lead to higher regurge.

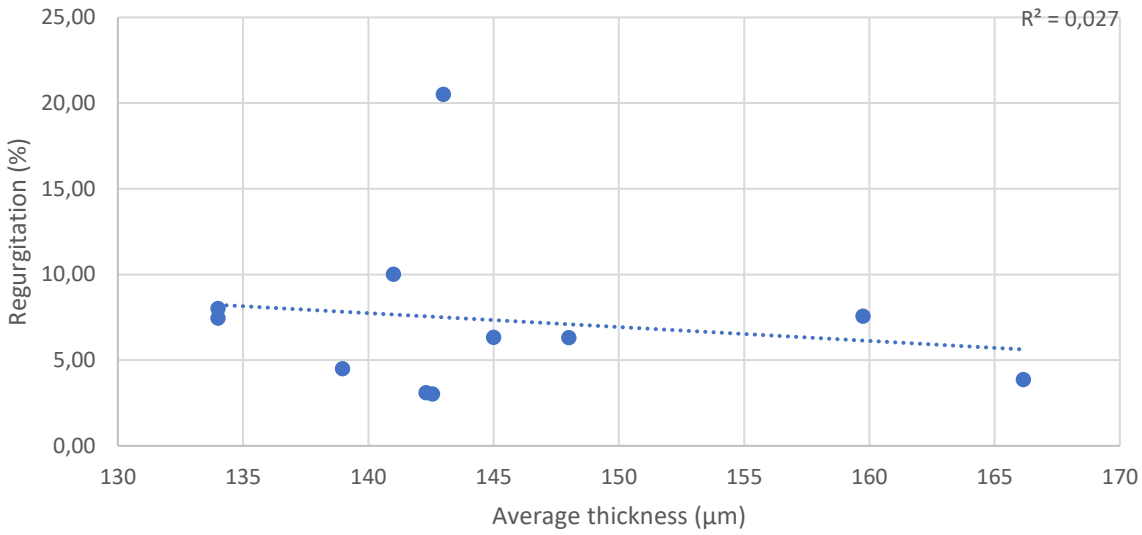

Figure 47 Average thickness vs regurgitation

There was no correlation between closing volume and thickness (R^2 = 0.24, p = 0.27) (Figure 48). This result showed that there must be other factors that influence closing volume more significantly. One of the factors could be that the valve leaflets were manufactured in a closed position. Thus, due to the shape memory of the polymer, both thick and thin leaflets revert to the closed position at the same speed.

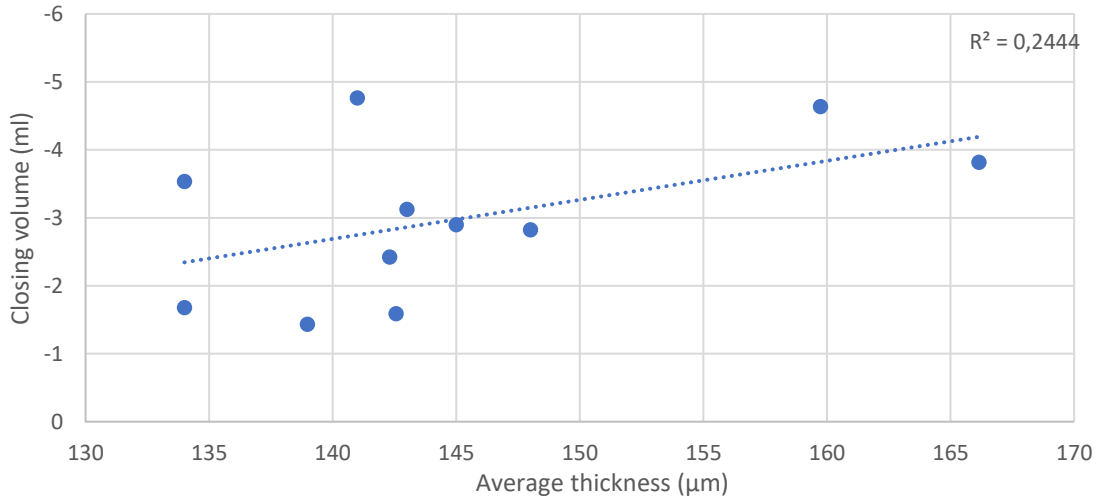

Figure 48 Average thickness vs closing volume.

Objectively there seemed to be some trend between leakage volume and thickness, but the R^2 value proved otherwise (0.13, p = 0.71) (Figure 49).

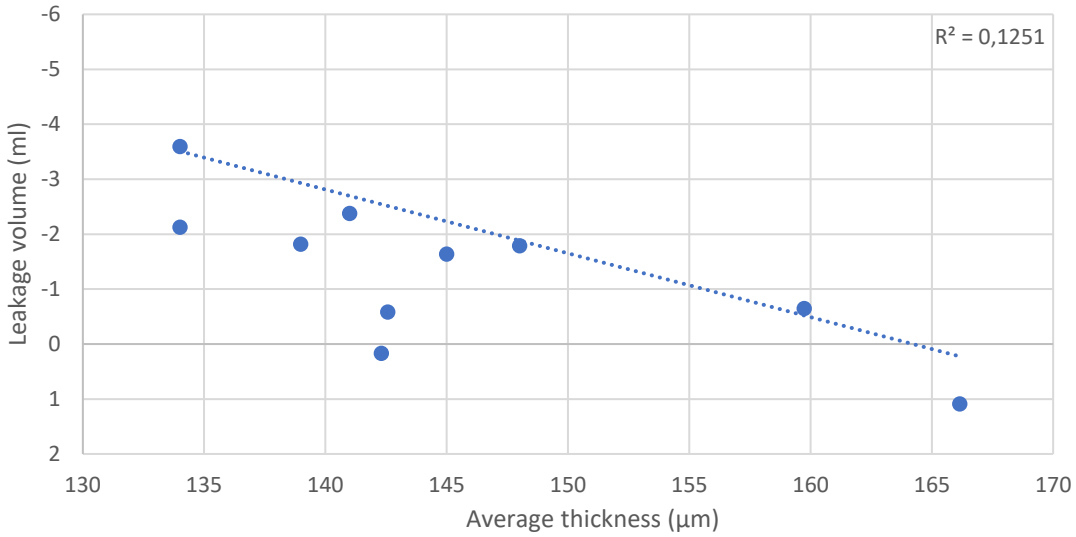

Figure 49 Average thickness vs leakage volume.

4.5 Durability

4.5.1 Durability Optimization

4.5.1.1 Initial Results

Initial valves that were manufactured had very low durability with average cycles until failure of 25.9 ± 20.8 million cycles. The valves all failed at the commissure post as seen in Figure 50.

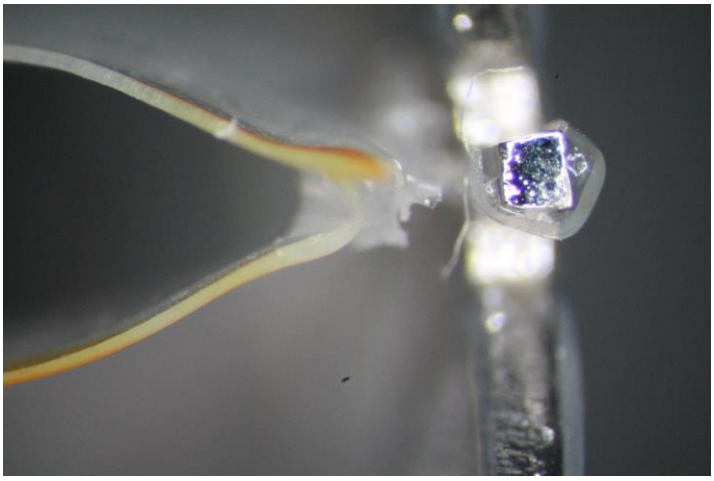

Figure 50 Polymer detaching from the metal at the top of the commissure post.

The repeated relative movement between the sharp edges of the stent probably caused the soft polymer to tear at this point, from where the leaflet tear propagates down the scallop.

4.5.1.2 Matchstick

Thickening up the top of the commissure was unsuccessful and decreased the average cycles until failure from 25.9 to 19.6 ± 13.5 million. The failure mechanism was the same as the non-matchsticked valves. The process of matchsticking is not easily reproducible and no improvement in durability was observed, thus matchsticking was not used in further studies.

4.5.1.3 Harder polymer pre-coat

The average cycles until failure for the harder polymer coated stents were 41.3 ± 59.4 million cycles. The standard deviation was large (59.4 million) with the minimum cycles being 0.2 million cycles and maximum cycles being 200.1 million.

The failure mechanism was different from the initial valves, with the harder durometer Carbosil 55D separating from the lower durometer Carbosil 80A. Upon further investigation, it was found that when the stent was positioned on the mould there was a very slight gap between the two (Figure 51), likely caused by the excessive force required to position the stent onto the mould with the extra polymer material present on the stent. This gap could explain the weak bond between the two hardness polymers.

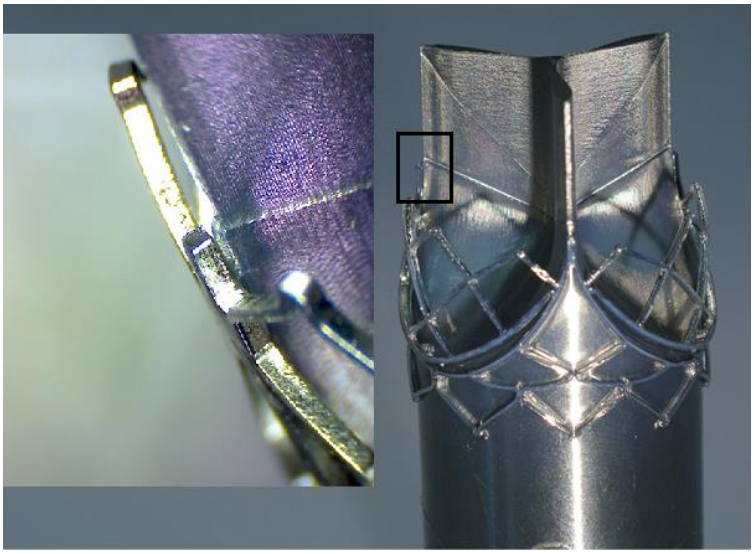

Figure 51 Stent lifting off the mould

4.5.1.4 Decreased Mould Size

An improvement was observed in the average cycles until failure of the smaller mould valves with mean cycles till failure of 167.9 ± 230.9 million, compared to the initial 25.9 ± 20.8. The

failure mechanism shifted from to the commissure post, to a tear that starts at the site where the strut extends out from the scallop of the stent (Figure 52)

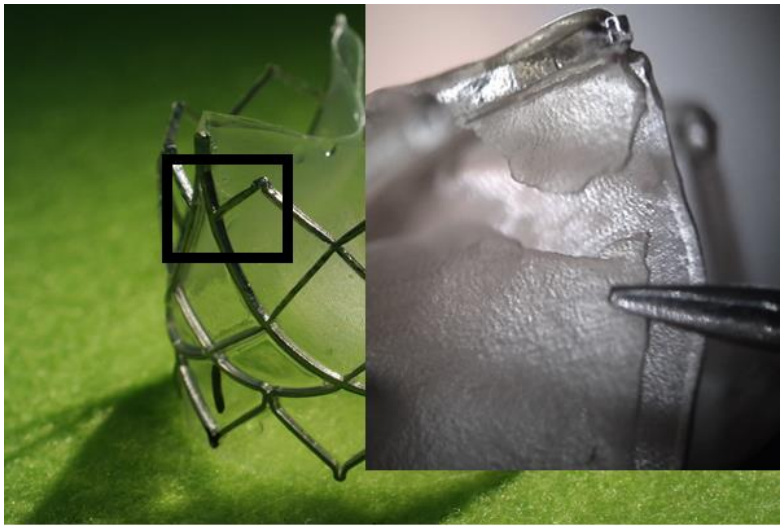

Figure 52 Tear starting underneath the arm and propagating upwards toward the free edge.

The reason for this failure site could be due to insufficient spray reaching underneath the stent strut, resulting in a thin polymer layer in that area. To investigate if this is the case, a valve was sent for thickness analysis using CT scanning (Figure 53). Results showed that wherever a strut extends from the scallop (purple lines), the leaflet was thinner than the rest of the valves.

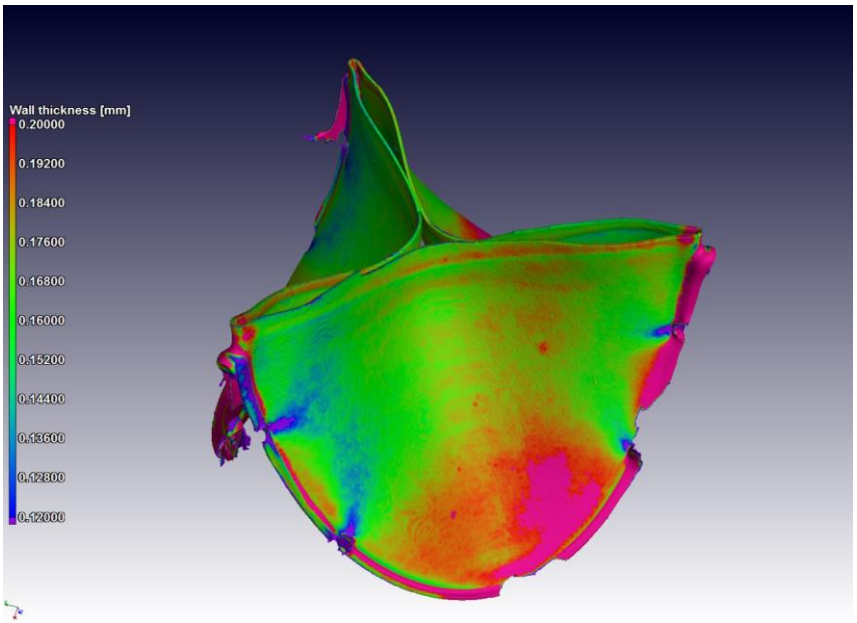

Figure 53 Thickness profile of valve leaflets using CT scanning. Clear thinner areas (purple) are seen where the arms of the stent are situated.

Figure 54 summarized the durability results from the different optimization steps. A clear improvement was seen at the last smaller mould optimization step, with one outlier reaching 600 million cycles.

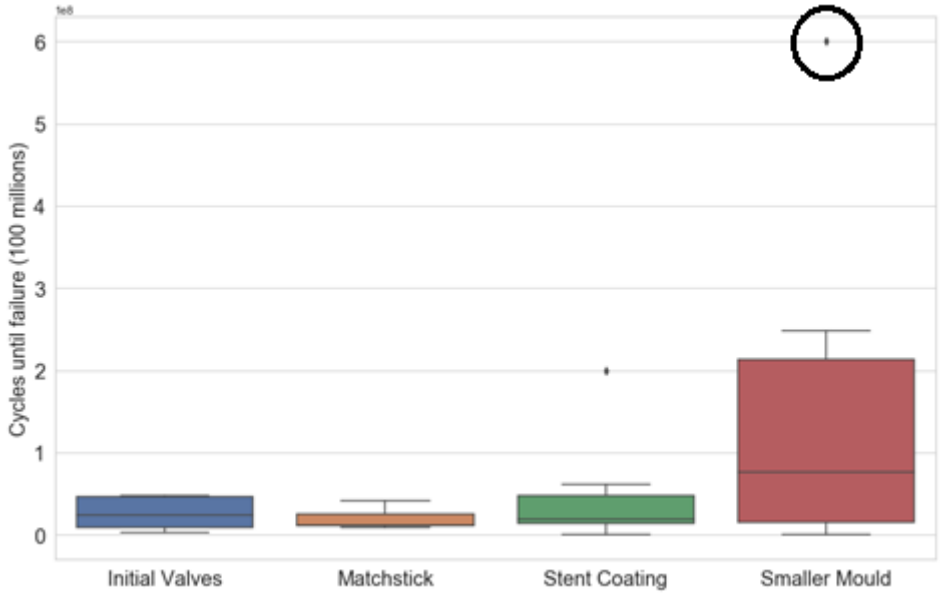

Figure 54 Cycles until failure in the fatigue tester for each optimization step.

4.5.1.5 Effect of thickness on durability

Cycles till failure of 150 million was chosen to represent a clear distinction between early valve failure and valves that showed promising longevity. Future work will use industry standards ISO 5840 (200 million cycles) as a benchmark. Valves that reached more than 150 million cycles were all concentrated in a narrow band of minimum, maximum, average thickness and below a certain standard deviation (Figure 55). The valves were concentrated between 150 and 180 µm maximum, 130 and 150 µm minimum and 140 and 160 µm average thickness. Also, all valves that exceeded past 150 million cycles had a standard deviation below 12.5 µm.

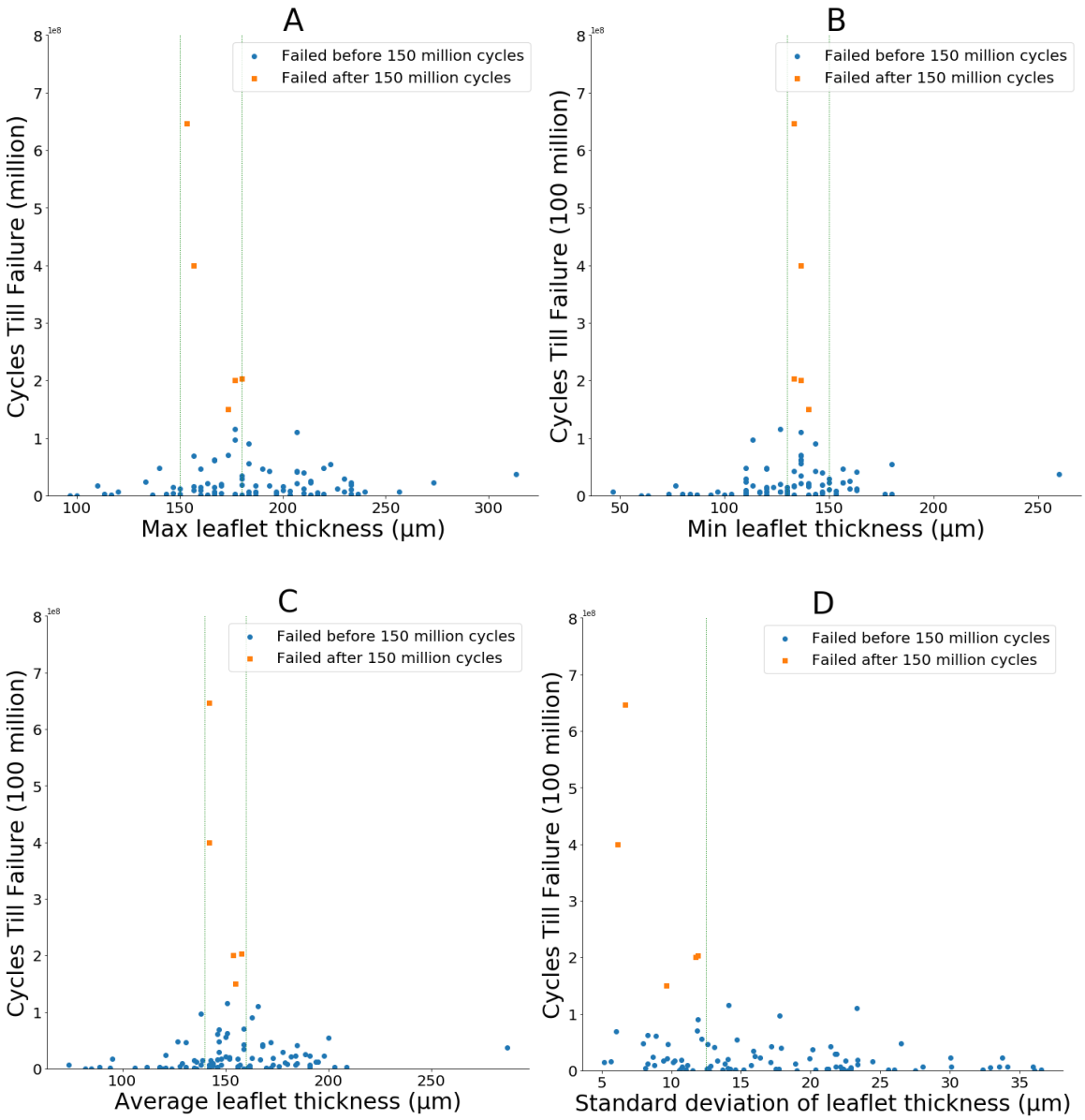

Figure 55 A: Maximum leaflet thickness B: Minimum leaflet thickness C: Average leaflet thickness and D: Standard deviation, all plotted against cycles till failure in FT.

The results summarized in Table 7 clearly showed the importance of thickness on the durability of the valves. Overall across all valves, it was shown that valves that had the preferred thickness distribution had a much better chance of increased durability (27.3% compared to 5.2%). Valves made with a smaller mould, with the hard polymer coating on the stent, and within the thickness criteria had 75 % of the samples reached more than 150 million cycles before failure. If the standard deviation criteria was further decreased to 10 µm the percentage of valves that reached 150 million cycles increased from 75 % to 100 %.

Table 7 Valve pass rate before and after applying thickness criteria.

Valves analyzed (total sample size and sample size of valves reached 150 million cycles)	**Valves exceeding 150 million cycles (% of total)**	**Valves with a preferred thickness exceeding 150 million cycles (% of total)**
All valves (n = 95, n = 11)	5.2 %	27.3 %
Smaller mould valves with 12.5 µm standard deviation criteria (n = 10, n = 4)	30 %	75 %
Smaller mould valves with 10 µm standard deviation criteria (n = 10, n = 3)	30 %	100 %

4.5.1 Fatigue tester validation

Valves tested in the PD had a GOA of 13.1± 2.5 % greater than the same valves tested in the FT. Meaning FT opened the valves slightly less compared to the PD.

4.6 Surface Roughness

The sprayed outflow surface had a R_a of 0.98 µm compared to 0.29 µm for the dip coated surface. A similar trend was seen in R_z values, with 3.95 µm compared to 1.09 µm measured for the outflow sides (Table 8). The inflow R_a and R_z were similar for both the manufacturing methods (Sprayed: $R_a = 1.04 \pm 0.18$, $R_z = 4.93 \pm 1.47$, Dipped: $R_a = 1.23 \pm 0.16$, $R_z = 5.84 \pm 1.87$).

Table 8 Surface roughness measurements for dip coated and sprayed valves.

	R_z (µm)	**R_a (µm)**
Dipped inflow	5.84 ± 1.87	1.23 ± 0.16
Dipped outflow	1.09 ± 0.10	0.29 ± 0.01
Sprayed inflow	4.93 ± 1.47	1.04 ± 0.18
Sprayed outflow	3.95 ± 0.98	0.98 ± 0.68

It was seen that dip casting inherently created a smooth surface layer, while it has been observed that spray coating creates a surface that is irregular and has crater like artifacts probably caused by random deposition of wet and dry droplets (Figure 56). The similar inflow surface roughness between the sprayed and dipped samples is due to the mould surface pattern being the same for both methods.

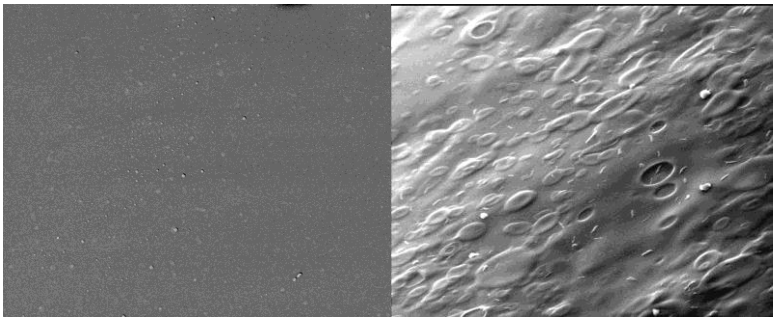

Figure 56 Surface micrographs of polymer valve samples, dipped (left), sprayed (right).

4.6.1 Final solvent spray

From the SEM pictures (Figure 57) it was clear that the surface roughness improved after solvent coating. The amount of solvent coating did not seem to make a significant difference. As expected the solvent dissolves the top layer of the polymer and creates a smooth surface after evaporation.

Figure 57 3x solvent spray (left) and 5x solvent spray (right)

4.7 ACUTE ANIMAL TRIAL

Adequate valve function was confirmed in vivo (Table 9), with an EOA of 1.60 cm^2. A temporary increase was seen 1 hour after implantation in the mean pressure gradient (1.01 to 10.27 mmHg), as well as an increase in heart rate (76 to 81 bpm). After 3 hours these measurements stabilized to 3.75 mmHg and 74 bpm respectively.

Table 9 Echo measurements before, immediately after and 3 hours after valve implantation.

Transaortic Echo measurements			
	Before	**After**	**3 hours**
P_{mean} (mmHg)	1.01	10.27	3.75
EOA (cm^2)	-	-	1.60
Heart rate (bpm)	76	91	74

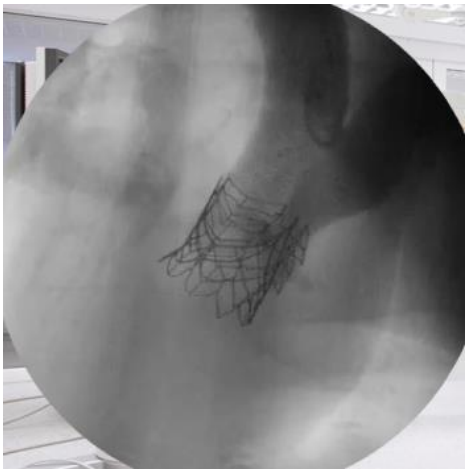

Figure 58 Contrast injection viewed on fluoroscopy.

The contrast injection showed no visible paravalvular or central regurgitation and that the coronary arteries were perfused (Figure 58). Visually the polymer leaflets showed no clear thrombus formation or any structural damage after explant (Figure 59). This is to be expected as thrombus and calcification will take much longer than 3 hours to happen and can only be tested using chronic animal implants.

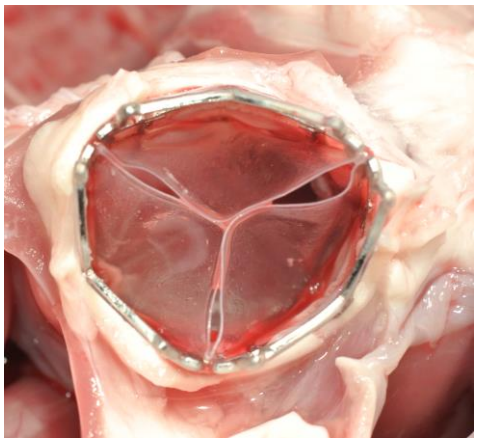

Figure 59 Explanted valve after the acute animal trial.

The temporary increase in pressure gradient could be due to the stress of the procedure elevating the heart rate and thus increasing the valve pressure gradient, or alternatively that the valve function improved over time due to leaflet swelling or softening due to temperature.

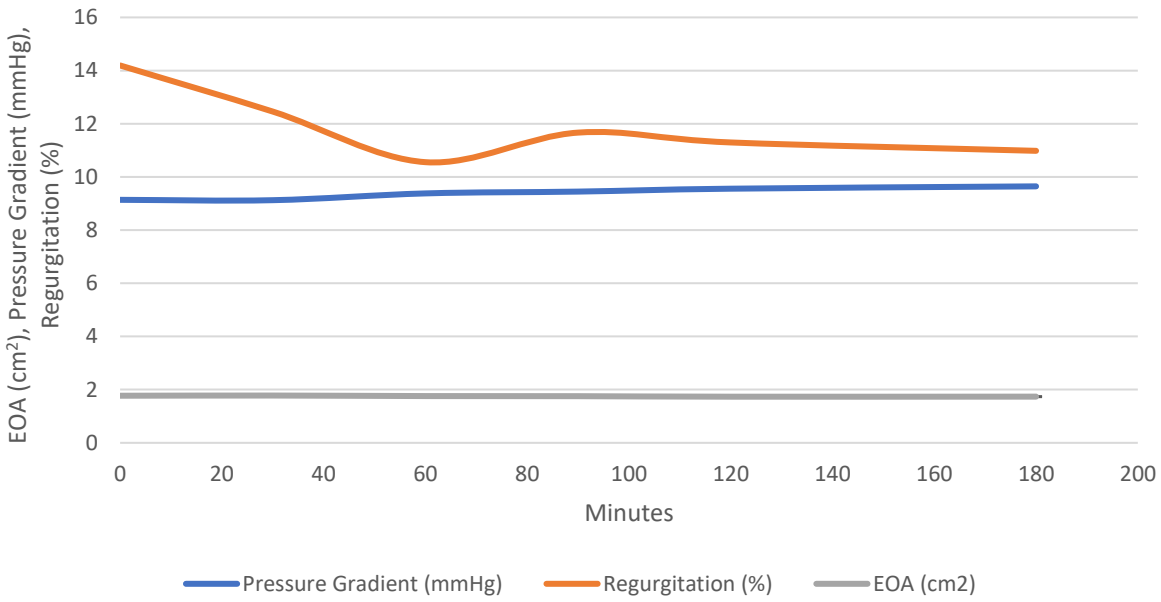

Figure 60 Valve function over time in the PD.

Testing in the PD showed a slight increase in pressure gradient (Figure 60) after 3 hours (9.1 to 9.6 mmHg). This contrasts with the observations in vivo, where a decrease from 10.27 to 3.75 mmHg was observed. There was a slight decrease in EOA (1.77 to 1.73 cm^2) and a decrease in regurge (14.20 to 11.00 %).

The pressure results from the PD seem to indicate that the temporary pressure gradient increase observed in the acute trial was due to the increase in heart rate and not the swelling of the valve leaflets or temperature decreasing the material modulus.

5 CONCLUSIONS

A spray process was used to successfully manufacture polymeric TAVI valves with leaflet thickness of 138 µm ± 17 µm.

The valves showed good hydrodynamic function (within ISO 5840:3 requirements) in terms of EOA (1.75 cm^2), pressure gradient (8.05 mmHg) and regurgitation (3.02 %).

Leaflet thickness indirectly linearly correlated to EOA and directly to pressure gradient. Interestingly no correlation between leaflet thickness and regurgitation was observed.

Manipulation of manufacturing methods and parameters resulted in 5 valves reaching in excess of 150 million cycles before failure in durability testing, with 1 of these reaching 600 million cycles (equating to 15 years in vivo function).

Leaflet thickness was found to be a good predictor of valve durability.

The polymeric TAVI valve performed well in acute ovine implantation, with retained coronary perfusion, no signs of paravalvular or central regurgitation and good function in terms of EOA (1.6 cm^2) and pressure gradient (3.75 mmHg).

6 RECOMMENDATIONS

The following recommendations for the further development of polymeric TAVI valves for improved valve function and durability are suggested:

1. A new automated spray rig with 6 axis control that is capable of reproducibly manufacturing valves with controlled leaflet thickness, while also allowing the nozzle to mould angle to be dynamically changed during coating is suggested. A robotic-arm based spray system could be a potential solution.
2. Cutting the free edge with an automated laser (CO_2 or excimer) system for improved consistency.
3. Chronic animal implants to assess thrombotic and calcification resistance of the polymer TAVI valves.

7 REFERENCES

1 Lutter, G., Ardehali, R., Cremer, J. & Bonhoeffer, P. Percutaneous Valve Replacement: Current State and Future Prospects. *The Annals of Thoracic Surgery* **78**, 2199-2206, doi:10.1016/j.athoracsur.2004.09.019 (2004).

2 Pinchuk, L. *et al.* Medical applications of poly(styrene-block-isobutylene-block-styrene) ("SIBS"). *Biomaterials* **29**, 448-460, doi:10.1016/j.biomaterials.2007.09.041 (2008).

3 Congenital Heart Disease (2018), https://www.nhs.uk/conditions/congenital-heart-disease/types/

4 Rock, C., Han, L. & Doehring, T. *Complex Collagen Fiber and Membrane Morphologies of the Whole Porcine Aortic Valve*. Vol. 9 (2014).

5 Tzemos, N. *et al.* Outcomes in adults with bicuspid aortic valves. *JAMA* **300**, 1317-1325, doi:10.1001/jama.300.11.1317 (2008).

6 Allison, M. A., Criqui, M. H. & Wright, C. M. Patterns and risk factors for systemic calcified atherosclerosis. *Arterioscler Thromb Vasc Biol* **24**, 331-336, doi:10.1161/01.ATV.0000110786.02097.0c (2004).

7 Mozaffarian, D. *et al.* Heart disease and stroke statistics--2015 update: a report from the American Heart Association. *Circulation* **131**, e29-322, doi:10.1161/CIR.0000000000000152 (2015).

8 Guilherme, L., Kalil, J. & Cunningham, M. Molecular mimicry in the autoimmune pathogenesis of rheumatic heart disease. *Autoimmunity* **39**, 31-39, doi:10.1080/08916930500484674 (2006).

9 Bland, E. F. & Duckett Jones, T. Rheumatic fever and rheumatic heart disease; a twenty year report on 1000 patients followed since childhood. *Circulation* **4**, 836-843 (1951).

10 Carapetis, J. R., Steer, A. C., Mulholland, E. K. & Weber, M. The global burden of group A streptococcal diseases. *Lancet Infect Dis* **5**, 685-694, doi:10.1016/S1473-3099(05)70267-X (2005).

11 Karthikeyan, G. *et al.* Rationale and design of a Global Rheumatic Heart Disease Registry: the REMEDY study. *Am Heart J* **163**, 535-540 e531, doi:10.1016/j.ahj.2012.01.003 (2012).

12 Mayosi, B. *et al.* The Drakensberg declaration on the control of rheumatic fever and rheumatic heart disease in Africa. *S Afr Med J* **96**, 246 (2006).

13 Marijon, E., Mirabel, M., Celermajer, D. S. & Jouven, X. Rheumatic heart disease. *Lancet* **379**, 953-964, doi:10.1016/S0140-6736(11)61171-9 (2012).

14 Osnabrugge, R. L. *et al.* Costs of transcatheter versus surgical aortic valve replacement in intermediate-risk patients. *Ann Thorac Surg* **94**, 1954-1960, doi:10.1016/j.athoracsur.2012.07.002 (2012).

15 Harken, D. E. *et al.* Partial and complete prostheses in aortic insufficiency. *The Journal of thoracic and cardiovascular surgery* **40**, 744-762 (1960).

16 Blackstone, E. H. Could it happen again? the Bjork-Shiley convexo-concave heart valve story. *Circulation* **111**, 2717-2719, doi:10.1161/CIRCULATIONAHA.105.540518 (2005).

17 Stein, P. D. *et al.* Antithrombotic therapy in patients with mechanical and biological prosthetic heart valves. *Chest* **102**, 445S-455S (1992).

18 Levine, M. N. & Hirsh, J. Hemorrhagic complications of anticoagulant therapy. *Semin Thromb Hemost* **12**, 39-57, doi:10.1055/s-2007-1003533 (1986).

19 Carpentier, A., Lemaigre, G., Robert, L., Carpentier, S. & Dubost, C. Biological factors affecting long-term results of valvular heterografts. *The Journal of thoracic and cardiovascular surgery* **58**, 467-483 (1969).

20 Cohn, L. H. *et al.* Fifteen-year experience with 1678 Hancock porcine bioprosthetic heart valve replacements. *Ann Surg* **210**, 435-442; discussion 442-433 (1989).

21 Schoen, F. J. & Levy, R. J. Calcification of tissue heart valve substitutes: progress toward understanding and prevention. *Ann Thorac Surg* **79**, 1072-1080, doi:10.1016/j.athoracsur.2004.06.033 (2005).
22 Hoffmann, G., Lutter, G. & Cremer, J. Durability of bioprosthetic cardiac valves. *Dtsch Arztebl Int* **105**, 143-148, doi:10.3238/arztebl.2008.0143 (2008).
23 Alizzi, A. M., Knight, J. L. & Tully, P. J. Surgical challenges in rheumatic heart disease in the Australian indigenous population. *Heart Lung Circ* **19**, 295-298, doi:10.1016/j.hlc.2010.02.010 (2010).
24 Edwards, M. B. & Taylor, K. M. Outcomes in nonagenarians after heart valve replacement operation. *Ann Thorac Surg* **75**, 830-834 (2003).
25 Iung, B. *et al.* Decision-making in elderly patients with severe aortic stenosis: why are so many denied surgery? *European heart journal* **26**, 2714-2720, doi:10.1093/eurheartj/ehi471 (2005).
26 Leon, M. B. *et al.* Transcatheter or Surgical Aortic-Valve Replacement in Intermediate-Risk Patients. *N Engl J Med* **374**, 1609-1620, doi:10.1056/NEJMoa1514616 (2016).
27 Rodes-Cabau, J. Transcatheter aortic valve implantation: current and future approaches. *Nature reviews. Cardiology* **9**, 15-29, doi:10.1038/nrcardio.2011.164 (2012).
28 Davies, H. CATHETER-MOUNTED VALVE FOR TEMPORARY RELIEF OF AORTIC INSUFFICIENCY. *The Lancet* **285**, 250, doi:10.1016/S0140-6736(65)91529-1.
29 Andersen, H. R., Knudsen, L. L. & Hasenkam, J. M. Transluminal implantation of artificial heart valves. Description of a new expandable aortic valve and initial results with implantation by catheter technique in closed chest pigs. *European heart journal* **13**, 704-708 (1992).
30 Pavcnik, D., Wright, K. C. & Wallace, S. Development and initial experimental evaluation of a prosthetic aortic valve for transcatheter placement. Work in progress. *Radiology* **183**, 151-154, doi:10.1148/radiology.183.1.1549662 (1992).
31 Bonhoeffer, P. *et al.* Transcatheter implantation of a bovine valve in pulmonary position: a lamb study. *Circulation* **102**, 813-816 (2000).
32 Boudjemline, Y. & Bonhoeffer, P. Steps toward percutaneous aortic valve replacement. *Circulation* **105**, 775-778 (2002).
33 Lutter, G. *et al.* Percutaneous aortic valve replacement: an experimental study. I. Studies on implantation. *The Journal of thoracic and cardiovascular surgery* **123**, 768-776 (2002).
34 Bonhoeffer, P. *et al.* Percutaneous replacement of pulmonary valve in a right-ventricle to pulmonary-artery prosthetic conduit with valve dysfunction. *Lancet* **356**, 1403-1405, doi:10.1016/S0140-6736(00)02844-0 (2000).
35 Cribier, A. *et al.* Percutaneous transcatheter implantation of an aortic valve prosthesis for calcific aortic stenosis: first human case description. *Circulation* **106**, 3006-3008 (2002).
36 Paniagua, D. *et al.* First human case of retrograde transcatheter implantation of an aortic valve prosthesis. *Tex Heart Inst J* **32**, 393-398 (2005).
37 Durko, A. P. *et al.* Annual number of candidates for transcatheter aortic valve implantation per country: current estimates and future projections. *European heart journal* **39**, 2635-2642, doi:10.1093/eurheartj/ehy107 (2018).
38 Vahl, T. P., Kodali, S. K. & Leon, M. B. Transcatheter Aortic Valve Replacement 2016: A Modern-Day "Through the Looking-Glass" Adventure. *J Am Coll Cardiol* **67**, 1472-1487, doi:10.1016/j.jacc.2015.12.059 (2016).
39 Ratner, B. D., Hoffman, A. S., Schoen, F. J. & Lemons, J. E. *Biomaterials Science: An Introduction to Materials in Medicine*. (Academic Press, 1996).
40 Roe, B. B. Late follow-up studies on flexible leaflet prosthetic valves. *The Journal of thoracic and cardiovascular surgery* **58**, 59-61 (1969).

41 Roe, B. B., Burke, M. F. & Zebner, H., Jr. The subcoronary implantation of a flexible tricuspid aortic valve prosthesis. *The Journal of thoracic and cardiovascular surgery* **40**, 561-567 (1960).
42 Mori, H. *et al.* Design and durability test of Silastic trileaflet aortic valve prostheses. *The Journal of thoracic and cardiovascular surgery* **65**, 576-582 (1973).
43 Gerring, E. L., Bellhouse, B. J., Bellhouse, F. H. & Haworth, W. S. Long term animal trials of the Oxford aortic/pulmonary valve prosthesis without anticoagulants. *Transactions - American Society for Artificial Internal Organs* **20 B**, 703-707 (1974).
44 Chetta, G. E. & Lloyd, J. R. The design, fabrication and evaluation of a trileaflet prosthetic heart valve. *Journal of biomechanical engineering* **102**, 34-41 (1980).
45 Yin, W. *et al.* Flow-induced platelet activation in a St. Jude mechanical heart valve, a trileaflet polymeric heart valve, and a St. Jude tissue valve. *Artificial Organs* **29**, 826-831, doi:DOI 10.1111/j.1525-1594.2005.29109.x (2005).
46 Gallocher, S. *Durability Assessment of Polymer Trileaflet Heart Valves* PHD thesis, Florida University, (2007).
47 Claiborne, T. E., Slepian, M. J., Hossainy, S. & Bluestein, D. Polymeric trileaflet prosthetic heart valves: evolution and path to clinical reality. *Expert Rev Med Devices* **9**, 577-594, doi:10.1586/erd.12.51 (2012).
48 Claiborne, T. E. *et al.* In vitro evaluation of a novel hemodynamically optimized trileaflet polymeric prosthetic heart valve. *Journal of biomechanical engineering* **135**, 021021, doi:10.1115/1.4023235 (2013).
49 Claiborne, T. E., Bluestein, D. & Schoephoerster, R. T. Development and evaluation of a novel artificial catheter-deliverable prosthetic heart valve and method for in vitro testing. *The International journal of artificial organs* **32**, 262-271 (2009).
50 Imamura, E. & Kaye, M. P. Function of expanded-polytetrafluoroethylene laminated trileaflet valves in animals. *Mayo Clin Proc* **52**, 770-775 (1977).
51 Braunwald, N. S. & Morrow, A. G. A Late Evaluation of Flexible Teflon Prostheses Utilized for Total Aortic Valve Replacement. Postoperative Clinical, Hemodynamic, and Pathological Assessments. *The Journal of thoracic and cardiovascular surgery* **49**, 485-496 (1965).
52 Nistal, F. *et al.* In vivo experimental assessment of polytetrafluoroethylene trileaflet heart valve prosthesis. *The Journal of thoracic and cardiovascular surgery* **99**, 1074-1081 (1990).
53 Szycher, M. *Szycher's handbook of polyurethanes*. (CRC Press, 1999).
54 Szycher, M. *Szycher's handbook of polyurethanes*. 2nd edn, (Taylor & Francis, 2013).
55 Zdrahala, R. J. & Zdrahala, I. J. Biomedical applications of polyurethanes: a review of past promises, present realities, and a vibrant future. *J Biomater Appl* **14**, 67-90 (1999).
56 Christenson, E. M., Anderson, J. M. & Hiltner, A. Oxidative mechanisms of poly(carbonate urethane) and poly(ether urethane) biodegradation:In vivo andin vitro correlations. *Journal of Biomedical Materials Research* **70A**, 245-255, doi:10.1002/jbm.a.30067 (2004).
57 Wu, Y. *et al.* An FTIR–ATR investigation of in vivo poly(ether urethane) degradation. *J Appl Polym Sci* **46**, 201-211, doi:doi:10.1002/app.1992.070460202 (1992).
58 Christenson, E. M., Dadsetan, M., Wiggins, M., Anderson, J. M. & Hiltner, A. Poly(carbonate urethane) and poly(ether urethane) biodegradation: in vivo studies. *Journal of biomedical materials research. Part A* **69**, 407-416, doi:10.1002/jbm.a.30002 (2004).
59 McBane, J. E., Santerre, J. P. & Labow, R. S. The interaction between hydrolytic and oxidative pathways in macrophage-mediated polyurethane degradation. *Journal of biomedical materials research. Part A* **82**, 984-994, doi:10.1002/jbm.a.31263 (2007).
60 Kidane, A. G. *et al.* Current developments and future prospects for heart valve replacement therapy. *Journal of biomedical materials research. Part B, Applied biomaterials* **88**, 290-303, doi:10.1002/jbm.b.31151 (2009).
61 Akutsu, T., Dreyer, B. & Kolff, W. J. Polyurethane artificial heart valves in animals. *J Appl Physiol* **14**, 1045-1048 (1959).

62 Ghista, D. N. & Reul, H. Optimal prosthetic aortic leaflet valve: Design parametric and longevity analyses: Development of the avcothane-51 leaflet valve based on the optimum design analysis. *Journal of biomechanics* **10**, 313-324, doi:http://dx.doi.org/10.1016/0021-9290(77)90004-5 (1977).
63 Wisman, C. B. *et al.* A polyurethane trileaflet cardiac valve prosthesis: in vitro and in vivo studies. *Transactions - American Society for Artificial Internal Organs* **28**, 164-168 (1982).
64 Hilbert, S. L., Ferrans, V. J., Tomita, Y., Eidbo, E. E. & Jones, M. Evaluation of explanted polyurethane trileaflet cardiac valve prostheses. *The Journal of thoracic and cardiovascular surgery* **94**, 419-429 (1987).
65 Kolff, W. J. & Yu, L. S. The return of elastomer valves. *The Annals of Thoracic Surgery* **48**, S98-S99, doi:10.1016/0003-4975(89)90658-9 (1989).
66 Deon Bezuidenhout, D. F. W., Peter Zilla. Polymeric heart valves for surgical implantation, catheter-based technologies and heart assist devices. *Biomaterials* **36**, 6-25 (2015).
67 Lo, H. B. *et al.* A tricuspid polyurethane heart valve as an alternative to mechanical prostheses or bioprostheses. *ASAIO Trans* **34**, 839-844 (1988).
68 Jansen, J. *et al.* Advances in design principle and fluid dynamics of a flexible polymeric heart valve. *ASAIO Trans* **37**, M451-453 (1991).
69 Daebritz, S. H. *et al.* Introduction of a flexible polymeric heart valve prosthesis with special design for mitral position. *Circulation* **108 Suppl 1**, II134-139, doi:10.1161/01.cir.0000087655.41288.dc (2003).
70 Daebritz, S. H. *et al.* New flexible polymeric heart valve prostheses for the mitral and aortic positions. *The heart surgery forum* **7**, E525-532, doi:10.1532/HSF98.20041083 (2004).
71 Schoen, F. J. Biomaterial-associated infection, neoplasia, and calcification. Clinicopathologic features and pathophysiologic concepts. *ASAIO Trans* **33**, 8-18 (1987).
72 Bernacca, G. M., Mackay, T. G., Wilkinson, R. & Wheatley, D. J. Calcification and fatigue failure in a polyurethane heart value. *Biomaterials* **16**, 279-285 (1995).
73 T.G Mackay, D. J. W., G.M. Bernacca, A.C Fisher, C.S. Hindle. New polyurethane heart valve prostheses design, manufacture and evaluation. *Biomaterials* **17**, 1857-1863 (1996).
74 Bernacca, G. M., Mackay, T. G., Wilkinson, R. & Wheatley, D. J. Polyurethane heart valves: fatigue failure, calcification, and polyurethane structure. *J Biomed Mater Res* **34**, 371-379 (1997).
75 Wheatley, D. J. *et al.* Polyurethane: material for the next generation of heart valve prostheses? *European journal of cardio-thoracic surgery : official journal of the European Association for Cardio-thoracic Surgery* **17**, 440-448 (2000).
76 Bernacca, G. M., Straub, I. & Wheatley, D. J. Mechanical and morphological study of biostable polyurethane heart valve leaflets explanted from sheep. *Journal of Biomedical Materials Research* **61**, 138-145, doi:10.1002/jbm.10149 (2002).
77 Bernacca, G. M., O'Connor, B., Williams, D. F. & Wheatley, D. J. Hydrodynamic function of polyurethane prosthetic heart valves: influences of Young's modulus and leaflet thickness. *Biomaterials* **23**, 45-50, doi:Doi 10.1016/S0142-9612(01)00077-1 (2002).
78 Haworth, W. S. Testing of Materials for Artificial Heart-Valves. *Brit Polym J* **10**, 297-301, doi:DOI 10.1002/pi.4980100414 (1978).
79 Bernacca, G. M., Mackay, T. G., Gulbransen, M. J., Donn, A. W. & Wheatley, D. J. Polyurethane heart valve durability: effects of leaflet thickness and material. *International Journal of Artificial Organs* **20**, 327-331 (1997).
80 Kidane, A. G. *et al.* A novel nanocomposite polymer for development of synthetic heart valve leaflets. *Acta biomaterialia* **5**, 2409-2417, doi:10.1016/j.actbio.2009.02.025 (2009).
81 Leat, M. E. & Fisher, J. A synthetic leaflet heart valve with improved opening characteristics. *Medical engineering & physics* **16**, 470-476 (1994).

82 Leat, M. E. & Fisher, J. The influence of manufacturing methods on the function and performance of a synthetic leaflet heart valve. *Proc Inst Mech Eng H* **209**, 65-69, doi:10.1243/PIME_PROC_1995_209_318_02 (1995).
83 D'Souza, S. S., Butterfield, M. & Fisher, J. Kinematics of synthetic flexible leaflet heart valves during accelerated testing. *J Heart Valve Dis* **12**, 110-119; discussion 119-120 (2003).
84 Rahmani, B., Tzamtzis, S., Ghanbari, H., Burriesci, G. & Seifalian, A. M. Manufacturing and hydrodynamic assessment of a novel aortic valve made of a new nanocomposite polymer. *Journal of biomechanics* **45**, 1205-1211, doi:10.1016/j.jbiomech.2012.01.046 (2012).
85 Kannan, R. Y. *et al.* The antithrombogenic potential of a polyhedral oligomeric silsesquioxane (POSS) nanocomposite. *Biomacromolecules* **7**, 215-223, doi:10.1021/bm050590z (2006).
86 Ghanbari, H. *et al.* The anti-calcification potential of a silsesquioxane nanocomposite polymer under in vitro conditions: potential material for synthetic leaflet heart valve. *Acta biomaterialia* **6**, 4249-4260, doi:10.1016/j.actbio.2010.06.015 (2010).
87 Kannan, R. Y., Salacinski, H. J., Odlyha, M., Butler, P. E. & Seifalian, A. M. The degradative resistance of polyhedral oligomeric silsesquioxane nanocore integrated polyurethanes: an in vitro study. *Biomaterials* **27**, 1971-1979, doi:10.1016/j.biomaterials.2005.10.006 (2006).
88 Sochman, J., Peregrin, J. H., Pavcnik, D., Timmermans, H. & Rosch, J. Percutaneous transcatheter aortic disc valve prosthesis implantation: A feasibility study. *Cardiovasc Inter Rad* **23**, 384-388, doi:DOI 10.1007/s002700010060 (2000).
89 Sochman, J. *et al.* Percutaneous transcatheter one-step mechanical aortic disc valve prosthesis implantation: A preliminary feasibility study in swine. *Cardiovasc Inter Rad* **29**, 114-119, doi:10.1007/s00270-005-0029-9 (2006).
90 Hashimoto, M. *et al.* Development of a Re-Positionable Aortic Stent-Valve: A Preliminary Study in Swine. *Journal of Interventional Cardiology* **21**, 432-440, doi:10.1111/j.1540-8183.2008.00393.x (2008).
91 Attmann, T., Steinseifer, U., Cremer, J. & Lutter, G. Percutaneous valve replacement: a novel low-profile polyurethane valved stent. *European journal of cardio-thoracic surgery : official journal of the European Association for Cardio-thoracic Surgery* **30**, 379, doi:10.1016/j.ejcts.2006.04.035 (2006).
92 Bianchi, M., Ghosh, R. P., Marom, G., Slepian, M. J. & Bluestein, D. Simulation of Transcatheter Aortic Valve Replacement in patient-specific aortic roots: Effect of crimping and positioning on device performance. *Conf Proc IEEE Eng Med Biol Soc* **2015**, 282-285, doi:10.1109/EMBC.2015.7318355 (2015).
93 Brubert, J. *et al.* Hemocompatibility of styrenic block copolymers for use in prosthetic heart valves. *Journal of materials science. Materials in medicine* **27**, 32, doi:10.1007/s10856-015-5628-7 (2016).
94 Sheriff, J. *et al.* Physical Characterization and Platelet Interactions under Shear Flows of a Novel Thermoset Polyisobutylene-based Co-polymer. *ACS Appl Mater Interfaces* **7**, 22058-22066, doi:10.1021/acsami.5b07254 (2015).
95 Rahmani, B. *et al.* In Vitro Hydrodynamic Assessment of a New Transcatheter Heart Valve Concept (the TRISKELE). *J Cardiovasc Transl Res*, doi:10.1007/s12265-016-9722-0 (2016).
96 Zhang, B. *et al.* Transcatheter Pulmonary Valve Replacement by Hybrid Approach Using a Novel Polymeric Prosthetic Heart Valve: Proof of Concept in Sheep. *PLoS ONE* **9**, e100065, doi:10.1371/journal.pone.0100065 (2014).
97 Wu, W. *et al.* Fluid-Structure Interaction Model of a Percutaneous Aortic Valve: Comparison with an In Vitro Test and Feasibility Study in a Patient-Specific Case. *Annals of biomedical engineering* **44**, 590-603, doi:10.1007/s10439-015-1429-x (2016).